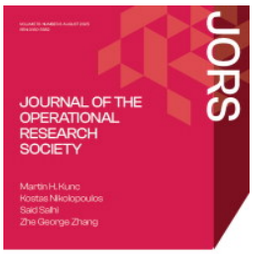

Journal of the Operational Research Society

ISSN: 0160-5682 (Print) 1476-9360 (Online) Journal homepage: www.tandfonline.com/journals/tjor20

A soft-constrained multi-objective facility location approach for designing a network of household waste recycling centres in South Yorkshire

Antonino Sgalambro, Serena Fugaro & Filippo Santarelli

To cite this article: Antonino Sgalambro, Serena Fugaro & Filippo Santarelli (31 Jul 2025): A soft-constrained multi-objective facility location approach for designing a network of household waste recycling centres in South Yorkshire, Journal of the Operational Research Society, DOI: 10.1080/01605682.2025.2537885

To link to this article: https://doi.org/10.1080/01605682.2025.2537885

© 2025 The Author(s). Published by Informa UK Limited, trading as Taylor & Francis Group

Published online: 31 Jul 2025.

Submit your article to this journal

Article views: 154

View related articles

View Crossmark data

Full Terms & Conditions of access and use can be found at
https://www.tandfonline.com/action/journalInformation?journalCode=tjor20

JOURNAL OF THE OPERATIONAL RESEARCH SOCIETY
https://doi.org/10.1080/01605682.2025.2537885

OPEN ACCESS Check for updates

A soft-constrained multi-objective facility location approach for designing a network of household waste recycling centres in South Yorkshire

Antonino Sgalambro[a], Serena Fugaro[b] and Filippo Santarelli[b]

[a]Analytics, Technology and Operations Department, Leeds University Business School, University of Leeds, Leeds, UK; [b]Institute for Applications of Calculus, National Research Council of Italy, Rome, Italy

ABSTRACT

In the UK Government's 25 Year Environment Plan, the location of municipal waste collection and recycling facilities plays a crucial role in achieving the Government's recycling targets. Economic pressures are forcing UK local authorities to reorganise the network of household waste recycling centres (HWRCs) with the dual aim of reducing high operating costs and achieving high user satisfaction, whilst meeting specific legislative requirements. It becomes then paramount to support the optimal design of these networks considering the needs of all the stakeholders involved. We fill this gap by proposing a novel multi-objective facility location problem in waste management (WM) which formalises the underlying real-world scenario for the city of Sheffield in South Yorkshire, and by developing a soft-constrained version of the resulting problem to more accurately capture the actual dynamics driving the network design process. The resulting Pareto Sets are efficiently explored by the robust variant of the AUGMEnted ε-CONstraint method, and a computational characterisation of the proposed model is provided with benchmark instances from a real-world case study. Finally, in-depth scenario and sensitivity analyses provide quantitative and qualitative insights to support strategic planning and decision-making.

ARTICLE HISTORY
Received 8 February 2024
Accepted 17 July 2025

KEYWORDS
Location; waste management; multi-objective optimisation; soft constraints; augmented ε-constraint; case study

1. Introduction

Waste minimisation appears among the objectives of the 25 Year Environment Plan drawn up in 2018 by the UK government, with the aim of "leaving the environment in better condition than it was" (His Majesty Government, 2018). At this purpose, the *Resource and Waste Strategy*, aimed at facilitating the transition to circular economy, sets an important target: achieving a municipal waste recycling rate of 65% by 2035 (Local Government Association, 2018). However, in 2020, the UK produced over 27,000 tonnes of waste of which only the 44.4% was recycled, according to the report of the Department of Environment, Food and Rural Affairs (DEFRA), which is in charge of waste management (WM) (DEFRA, 2020).

At the local level, WM is delegated to British local authorities (LA), which are responsible for collecting, recycling, or incinerating waste. The *household waste recycling centres* (HWRCs) play a key role in this. These centres receive massive quantities of selected materials and provide residents with a service for re-use or recycling, as well as for the collection of any waste that cannot be collected – or is not economically viable – by the door-to-door system (WRAP, 2018a, 2018b). In particular, at HWRCs, waste is separated and then transported by lorry for further processing or disposal to end points such as recycling facilities, incinerators, landfills, Energy Recovery Facilities, and Waste Transfer Stations. Specifically, the performance of these centres is measured by two components: the recycling rates and the site-users satisfaction, both influenced by the location, layout and service provided by site staff (Zaharudin et al., 2021). Indeed, staff are responsible for the efficient operation of the centres as well as for a good user experience: well-trained and helpful staff have a positive impact on the recycling rate (WRAP, 2018b). Moreover, the network of HWRCs is generally developed with a strong focus on accessibility. Indeed, the National Assessment of Civic Amenity Sites (NACAS) has set out the fundamental criteria to be considered when deciding where to locate these facilities. These criteria include recommending maximum catchment radii and the driving times to a site for both urban and rural areas, as well as the minimum number of sites per residents (WRAP, 2018a).

However, DEFRA recently reported that the British LA had failed to reach the minimum threshold of 50% recycled/reused waste set up by government (DEFRA,

CONTACT Antonino Sgalambro a.sgalambro@leeds.ac.uk Analytics, Technology and Operations Department, Leeds University Business School, University of Leeds, UK

© 2025 The Author(s). Published by Informa UK Limited, trading as Taylor & Francis Group
This is an Open Access article distributed under the terms of the Creative Commons Attribution-NonCommercial-NoDerivatives License (http://creativecommons.org/licenses/by-nc-nd/4.0/), which permits non-commercial re-use, distribution, and reproduction in any medium, provided the original work is properly cited, and is not altered, transformed, or built upon in any way. The terms on which this article has been published allow the posting of the Accepted Manuscript in a repository by the author(s) or with their consent.

2019). Such an outcome relies on several critical aspects, as underlined in the recent survey by Oluwadipe et al. (2022). Namely, beyond the physical barriers and the lack of public engagement in recycling operations, another factor that challenges the efficient functioning of the HWRCs network is the economic one. In fact, the UK public sector is affected by continuous funding cuts; additionally, considerable resources are necessary to attain increasing recycling rates. Thus, LA face significant challenges in providing a high level and cost-effective service (Smith & Bolton, 2018; Zaharudin et al., 2022). As a result, some of them are opting to close facilities, although this is not advisable as it would inevitably lead to greater affluence of the remaining facilities, with consequent user dissatisfaction, potentially increasing *fly-tipping* (i.e., illegal dumping of waste) and reducing the recycling rates (Smith, 2023).

In this context and facing similar issues, the City Council of Sheffield, in South Yorkshire, would like to explore different configurations of its actual HWRCs network. In fact, Sheffield is one of the cities in England where the financial pressure suffered by LA has severely affected WM services, causing considerable discomfort to citizens (BBC, 2016). Moreover, Sheffield's HWRCs only accept bulky waste, so they are accessible only by car, and have limited collection capacity, which can increase lead times and cause frequent traffic congestion on the surrounding roads (Engkvist et al., 2016; Zaharudin et al., 2022).

With these critical issues in mind, Sheffield City Council aims at enhancing its current HWRCs network by exploring novel configurations which meet NACAS requirements, while enabling the pursuit of strategic objectives such as reducing overall running costs and improving service quality. Actually, the decision-making process underlying such network design operations should be implemented with a holistic approach accounting for the needs of diverse stakeholders involved: installers and users. Indeed, including the needs of householders, who are the beneficiaries of the service, in the design evaluation process could be beneficial in achieving higher recycling rates (De Feo & De Gisi, 2010).

Mathematically, the adoption of this multi-stakeholder perspective leads to the use of multi-objective tools. Indeed, this approach has been used to investigate several WM location problems in the related literature (Adeleke & Olukanni, 2020; Fugaro & Sgalambro, 2025). Among others, Alumur and Kara (2007) proposed a Bi-Objective Location-Routing problem for hazardous waste. The objective is to determine the optimal locations for treatment and disposal facilities, as well as the quantities of hazardous waste to be transported, with the dual aim of minimising both the *overall costs*, obtained by summing the costs of transport, treatment and disposal operations, and the *transportation risk*, measured with population exposure. Similarly, both Samanlioglu (2013) and Zhao et al. (2016) tackled the problems of locating hazardous waste recycling, treatment and disposal centres, and of routing different typologies of waste between specific centres, aiming to minimise overall costs and risks, both related to transport and location processes. Recently, Wang et al. (2021) addressed a similar Location-Routing problem, and included maximising household convenience as an objective, to achieve greater participation in the collection phase. Specifically, the *convenience score* is measured by a non-decreasing function of user-site distance. Focusing on increasing the e-waste market capture through advertising, Shi et al. (2020) developed a Bi-Objective model to locate *Waste Electrical and Electronic Equipment* (WEEE) centres in Changsha (China). Specifically, the two conflicting objectives considered are maximising the amount of e-waste collected from customers and minimising the total cost of installation and advertisement. Instead, Ahluwalia & Nema (2011) proposed a multi-objective and multi-period approach to a location and capacity planning for WEEE centres, where the decisions also concern the allocation of waste to different types of facilities (e.g., storage, disposal, and recycling) while minimising four objectives: transportation and operating costs, environmental risk, socially perceived risk and health risk. Erkut et al. (2008) addressed a Location–Allocation problem for municipal Solid WM in North Greece. The objectives encompass: the minimisation of greenhouse effect, the minimisation of final disposal to landfill, the minimisation of overall costs (installation, treatment, and transport), and the maximisation of both energy recovery from sanitary landfills and incinerators, and material recovery. Instead, Darmian et al. (2020) modelled the location of Municipal Solid Waste collection centres in Iran integrating districting decisions. They formulated three objectives reflecting economic, environmental, and social criteria: minimisation of establishment and waste collection costs; minimisation of destructive environmental impacts, quantified through emissions from construction and pollution caused by transport; minimisation of social dissatisfaction. Similarly, Shokouhyar and Aalirezaei (2017) described a Tri-Objective Location-Allocation model for the design of a WEEE reverse logistics network in Iran. The objectives are: to maximise profit, expressed as the difference between the revenue generated from selling recovered materials and the costs of setting up and operating the WEEE network; to maximise the social impact of the network in terms of employment and regional development; to minimise negative environmental impacts, measured as

pollution from transport. Kailomsom and Khompatraporn (2023) addressed a problem of Infectious Waste Transshipment and Disposal in Thailand using a multi-objective approach. This involved defining three objective functions to represent the economic, environmental and social impacts of such a system: minimising installation and transport costs; minimising the amount of neighbouring population within a certain distance from the disposal facilities; minimising CO_2 emissions from the transshipment and disposal facilities. Similarly, to address an Infectious waste disposal centres location problem, Wichapa and Khokhajaikiat (2017, 2018) defined a bi-objective location-routing problem, including different social and environmental criteria to select the location of candidate centres while minimising the costs of installation, operation and transport. Also, Zhao et al. (2021) applied a bi-objective approach to a Location-Routing problem in the field of Infectious WM. Specifically, the authors accounted for the stochastic nature of waste generation during a pandemic and proposed a scenario-based robust optimisation model. The objectives considered address both economic costs and the risks associated with the handling and transportation of infectious waste. Tralhão et al. (2010) addressed the problem of identifying the location and capacity of multi-compartment containers for urban-sorted waste in Coimbra. They considered four objectives: minimising the costs of the facilities, minimising the average user-site distance, minimising the number of users too close to a container or too far away from the respective multi-compartment container. Tari & Alumur (2014) addressed a similar problem for WEEE collection centres in Turkey in the context of reverse logistics. The authors proposed a Tri-Objective Location-Allocation problem where the objectives are: minimising the overall costs (installation and transport), minimising the maximum difference in surplus materials sent to different companies (to ensure *equity*), minimising the maximum deviation from the mean demand (to ensure prompt supply of products to each company). Finally, to meet the needs of both the government and the sanitation companies, Ma et al. (2021) proposed a bi-level bi-objective location-routing model for Municipal WM. In particular, the *leader*, i.e., the government, pursues several conflicting objectives concurrently: minimising the obnoxious effects, along with opening and handling costs for facilities and vehicle costs.

As can be inferred from the above contributions, multi-objective WM location problems generally feature an economic objective, e.g., minimising the costs of installing and/or operating the facilities. As for the others, they depend on the managerial context underlying the decision-making process. However, although the need for this multi-stakeholder approach has been recognised (DEFRA, 2019), up to our knowledge, no paper has yet adopted a Multi-Objective perspective to formulate the aforementioned UK-specific network design problem. Therefore, in this article, we introduce and model an original multi-objective facility location problem for the design of the HWRCs network in Sheffield.

Specifically, the contribution of our research is at the strategic level: its aim is to help the decision-maker to locate a maximum number of facilities with a given capacity and to allocate citizens (i.e., users) accordingly, taking into account their preference to be served by the nearest centre. Indeed, the decision process is guided by the pursuit of two objectives: minimising overall costs and maximising service quality. As a novelty with respect to the general approach in the literature for this type of network design problems (Habibi et al., 2017; Wichapa & Khokhajaikiat, 2017), where the facility location and demand allocation costs are usually minimised together, we formulate them as different objectives to be optimised. This reflects the respective perspectives of facility installers and users. Another innovative aspect of the proposed model is that it decomposes the maximisation of service quality into two distinct and potentially conflicting objectives. Not only do we present it from the users' perspective, focusing on the distance to the nearest active centre, but we also model a coverage function to measure how the HWRCs network complies with the legislative requirements regarding the distance between users and sites (WRAP, 2018a). In addition, capacity flexibility of the facilities was identified as one of the key elements to enable the handling of visitor peaks and to avoid the creation of bottlenecks (Engkvist et al., 2016). However, to the best of our knowledge, this aspect has not been explored in the literature on WM Facility Location problems, which has mainly focused on capacity planning at the strategic level (Ahluwalia & Nema, 2011; Tari & Alumur, 2014). Therefore, we also propose a *soft-constrained* approach to the design of the HWRCs network in Sheffield, by allowing the capacity constraints to be violated when allocating demand. Both the managerial and computational implications of such relaxed constraints have been extensively studied. Specific contributions of this research are summarised below:

- the definition of a novel multi-objective location problem in WM, characterised by the innovative combination of different managerial perspectives arising from a real-world case study in the city of Sheffield;
- the complexity characterisation along with a mathematical formulation for the emerging

problem, obtained through Integer Linear Programming tools and featuring original reformulation of classic constraints;
- the development of a soft-constrained version of the problem by allowing the realistic violation of a particular class of constraints;
- the exact yet efficient exploration of the arising Pareto Sets through the robust version of the Augmented ε-constraint framework, i.e., AUGMECON-R (Nikas et al., 2022);
- a thorough computational experimentation – conducted on benchmark instances, obtained from real data – aimed at providing quantitative and qualitative insights into the resulting different configurations for the HWRCs network design;
- the construction and analysis of a real-world case study, aimed at providing a feasibility study of the network reconfiguration process using the proposed models.

To favour an effortless understanding of the new problem framework and its modelling features, Section 2 first introduces the Multi-Objective Household Waste Recycling Centres HWRCs Location Problem. Section 3 then presents and thoroughly analyses the computational experiments conducted on the benchmark instances obtained from real-world data for the city of Sheffield. Section 4 introduces the soft-constrained approach to the problem, providing the mathematical formulation devised and reporting the related computational experiments. Section 5 provides the in-depth scenario and sensitivity analyses of a real case study for the city of Sheffield, offering concrete managerial insights to support strategic planning and decision-making. Section 6 concludes with recommendations for future research.

2. The multi-objective household waste recycling centres location problem

This section introduces a multi-objective facility location problem for the design of a HWRCs network, hereafter referred to as HWRC-Loc. Specifically, Section 2.1 provides a description of the problem, along with a study of its computational complexity, while Section 2.2 details an ad-hoc multi-objective integer programming formulation devised for it.

2.1. Problem description

We suppose that it is deemed necessary to design the network of HWRCs for a region, either geographical or political. Specifically, a set of HWRC facilities must be located in order to meet certain legislative, economic, and service requirements for that region. Additionally, we assume that citizens have been grouped into disjoint subsets, called *cells*, according to their position (Ghiani et al., 2012). Indeed, depending on the population density, a cell may consist of a single dwelling or of several districts. We also make the realistic assumption that only a limited amount of waste can be collected at a HWRC.

To formally state the problem let $G = (N, E)$ be an undirected graph, with $N = I \cup J$, and $I \cap J = \emptyset$, where I represents the set of *demand nodes*, and J the set of *facility sites* for the location of HWRCs. In particular, the demand nodes correspond to the cells, considered as point sources, i.e., each cell is identified by its centroid; hence, in the following, the terms cell and demand node are interchangeable. Then, h_i is the *demand* of node i, e.g., it is the number of citizens grouped in cell $i \in I$; r_j is the non-negative *running cost* of $j \in J$, and c_j is the non-negative *capacity* of $j \in J$, i.e., the number of citizens that can be served by facility located at $j \in J$.

Besides, at most P facilities can be located, and $E = I \times J$ contains all the edges defining the potential *assignment* of demand nodes to facility sites, i.e., all citizens belonging to the cell are assigned to the same HWRC. Then, d_{ij} is the distance between the demand node $i \in I$ and the facility site $j \in J$. To model the legislative requirements, we assume that the authority designing the network has set a threshold for the maximum distance between a cell and the centre to which it is assigned.

Definition 2.1. *A demand node is "covered" if it is assigned to a facility located within a threshold distance D.*

In particular, $N_i = \{j \in J | d_{ij} \leq D\}$ denotes the set of facility sites which can cover demand node i. By assumption, the *single allocation hypothesis* holds (Daskin, 2011), so a demand node can be assigned to exactly one located facility, namely the closest one. Table 1 summarises the notations introduced so far.

The HWRC-Loc is based on the following two decisions:

Table 1. Notations for the formal description of the HWRC-Loc.

Sets		Function values		Parameters	
I	demand nodes (cells)	c_j	capacity for $j \in J$	P	max number of facilities to be located
J	facility sites (HWRCs)	r_j	running cost for $j \in J$	D	threshold value for coverage distance
E	edges connecting nodes of I and J	h_i	value of demand at $i \in I$		
N_i	sites not further than D from i	d_{ij}	distance between $i \in I$ and $j \in J$		

- selection of at most P facilities (HWRCs) to be located in the region;
- allocation of demand nodes (cells) to the closest located facilities while jointly satisfying capacity limitations.

The fulfilment of the following multiple objectives guides the decision-making process:

1. minimisation of the total running costs;
2. minimisation of the total distance between facility sites and their assigned demand nodes;
3. maximisation of the total covered demand.

From a managerial perspective, (1) deals with the cost of the service network, while (2) and (3) relate to service quality. It is worth highlighting the following innovative aspects which distinguish the multi-objective approach we propose to this problem from the existing literature on facility location problems in WM. On the one hand, we decouple the costs associated with the location of facilities and the allocation of demand, since these types of costs need to be optimised separately in order to properly represent the interests of two different stakeholders involved in this network design problem, i.e., service providers and service users. On the other hand, we assess the service quality of the HWRCs network not only in terms of user satisfaction but also in terms of its compliance with legislative requirements; again this is a means to taking into account the different and potentially conflicting interests that guide the installation of the HWRC facilities.

Lemma 2.2. *The HWRC-Loc is an NP-hard problem.*

Proof. Suppose that the running cost function is null so that exactly P facilities can be located at no cost. Therefore, the HWRC-Loc becomes a Capacitated p *-median-cover Problem* (Sáez-Aguado & Trandafir, 2018) with closest assignment constraints (CACs). Assuming that the distance function is identically equal to 1 and that the threshold value D is at least equal to 2, then each demand node can be covered by any located facility, and the CAC are satisfied by any choice of facility sites.

Since the (Capacitated) p-median-cover Problem can be reduced to a classic (Capacitated) p-median Problem (Daskin, 2011) which has been proven NP-hard (Garey & Johnson, 1979), the same computational result holds for the HWRC-Loc. ■

2.2. An integer linear programming model

The proposed model relies on the use of the following sets of variables:

1. binary *facility location* variables x_j, defined $\forall j \in J$, such that $x_j = 1$ if a facility is located in j, and 0 otherwise;
2. binary *assignment* variables y_{ij}, defined $\forall i \in I, \forall j \in J$, such that $y_{ij} = 1$ if demand node i is assigned to facility in j, and 0 otherwise;
3. binary *coverage* variables z_i, defined $\forall i \in I$, such that $z_i = 1$ if demand node i is covered, and 0 otherwise.

The three objectives pursued in the decision-making process, as described in Section 2.1, are formalised through the following functions:

1. $\mathcal{RC} = \sum_{j\in J} r_j x_j$ denoting the overall running costs;
2. $\mathcal{UC} = \sum_{i\in I}\sum_{j\in J} h_i d_{ij} y_{ij}$ representing the *user costs*, i.e., the sum of the demand-weighted distances between the located facilities and the demand nodes assigned to them;
3. $\mathcal{CO} = \sum_{i\in I} h_i z_i$ denoting the covered demand.

It is worthwhile emphasising that the HWRC-Loc is intrinsically multi-objective given the inherently conflicting nature of the goals to be pursued. In fact, the trend of $\mathcal{RC}$ is opposite to that of the remaining objectives, in that it is negatively affected by an increased number of located facilities whilst this could be beneficial for both $\mathcal{UC}$ and $\mathcal{CO}$ values. However, since the aggregation criterion for citizens results in possibly non-uniform distributed demand values, minimising $\mathcal{UC}$ may also be in conflict with maximising $\mathcal{CO}$. See Appendix A for a more rigorous explanation drawing on some evidence supporting this thesis.

The resulting multi-objective integer linear program is given by (1) in which (1a) minimises the total running costs, (1b) minimises the user costs, and (1c) maximises the covered demand.

$$\text{(HWRC-Loc)} \quad \min \ \mathcal{RC} \tag{1a}$$
$$\min \ \mathcal{UC} \tag{1b}$$
$$\max \ \mathcal{CO} \tag{1c}$$

subject to

$$\sum_{i\in I} h_i y_{ij} \le c_j x_j \quad \forall j \in J \tag{1d}$$
$$\sum_{j\in J} x_j \le P \tag{1e}$$
$$\sum_{j\in J} y_{ij} = 1 \quad \forall i \in I \tag{1f}$$
$$\sum_{\{a:d_{ia}\le d_{ij}\}} y_{ia} \ge x_j \quad \forall i \in I, \forall j \in J \tag{1g}$$
$$z_i \le \sum_{j\in N_i} x_j \quad \forall i \in I \tag{1h}$$
$$x_j, y_{ij}, z_i \in \{0,1\} \quad \forall i \in I, \ \forall j \in J \tag{1i}$$

Constraints (1d) couple the *capacity requirements* with the *activation constraints*, stating that demand covered by any located HWRC facility cannot exceed its capacity. Constraint (1e) states that at most P facilities can be located, whilst those (1f) represent the *single allocation* conditions, stating that each cell has to be assigned to exactly one facility, which has to be the closest located facility according to the CAC (1 g). Then, Constraints (1h) are the *coverage constraints* stating that a demand node is covered whenever a facility is located within distance D from it. Finally, Constraints (1i) are binary constraints for variables. The resulting model encompasses: $|I| + |J| + |I||J|$ binary variables, and $2|J|(|I| + 1) + 3|I| + 1$ linear constraints.

Remark 1. It should be emphasised that, while the minimisation of the $\mathcal{UC}$ function is instrumental at assessing the service quality from the users perspective, the CAC are essential to represent their behaviour (Ghiani et al., 2012). In fact, in the specific operational setting considered in this paper, there is no possibility of inducing users to choose a particular centre (Zaharudin et al., 2021). Therefore, the CAC are hard constraints aimed at expressing the users' preference to go to the active centre closest to the cell to which they belong.

In particular, the $\mathcal{O}(|N|^2)$ equations in (1 g) were introduced by Church and Cohon (1976), whilst Espejo et al. (2012) proved that they are valid in case of ties for distances between demand nodes and facilities, independently from Constraints (1e). However, in Theorem 2.3 we proved that the CAC can be equivalently stated with the original $|J|$ constraints in (2):

$$\sum_{i \in I} \sum_{\{a : d_{ia} \leq d_{ij}\}} y_{ia} \geq |I| x_j \qquad \forall j \in J. \tag{2}$$

Theorem 2.3. *If (1f) and (1i) hold, then Constraints (1g) and (2) are equivalent.*

Proof. (1g) $\Rightarrow$ (2) follows by summing (1 g) over I.

Conversely, define the variables $A_{ij} = \sum_{\{a : d_{ia} \leq d_{ij}\}} y_{ia}$, and observe that $0 \leq A_{ij} \leq 1$, $\forall i \in I$ and $\forall j \in J$. Indeed, the former inequality follows from the integrality conditions for variables y, while the latter relies on Constraints (1f). Then (2) $\Rightarrow$ (1g) if for any fixed $j \in J$ it holds that:

$$A_{ij} \geq x_j \qquad \forall i \in I \tag{3}$$

Suppose that there exists a $\hat{j} \in J$ such that (3) do not hold: then, there must exist at least one $\hat{i} \in I$ such that $A_{\hat{i}\hat{j}} < x_{\hat{j}}$. Indeed, the integrality conditions (1i) of the x variables and the non-negativity of the A variables, imply that $x_{\hat{j}} = 1$ and $A_{\hat{i}\hat{j}} = 0$. Since $A_{\hat{i}\hat{j}} \leq 1$ $\forall i \in I$, the sum of the $A_{\hat{i}\hat{j}}$ variables verifies the following inequality:

$$\sum_{i \in I} A_{\hat{i}\hat{j}} = \sum_{i \in I \setminus \{\hat{i}\}} A_{\hat{i}\hat{j}} \leq |I| - 1 \tag{4}$$

Moreover, by hypothesis, the Constraints (2) hold, thus for $\hat{j}$ we have that:

$$\sum_{i \in I} A_{\hat{i}\hat{j}} = \sum_{i \in I \setminus \{\hat{i}\}} A_{\hat{i}\hat{j}} \geq |I| x_{\hat{j}} = |I| \tag{5}$$

Combining Equations (4) and (5), we obtain $|I| \leq |I| - 1$ which is impossible. ■

Therefore, we replaced Constraints (1 g) with those (2), in our integer linear program, since they are equivalent but fewer. In particular, the resulting model encompasses $3(|J| + |I|) + |I||J| + 1$ linear constraints.

3. Computational experiments

This section presents the numerical experiments conducted with a twofold objective: to test the validity of the proposed model and to address the specific needs arising in a real case study. As the HWRC-Loc in inherently multi-objective, we adopted AUGMECON-R, the robust version of the AUGMEnted ε-CONstraint method (Nikas et al., 2022), to explore accurately the Pareto Sets, i.e., the set of efficient solutions. As detailed in Appendix B, this method iteratively solves a Single-Objective Problem (SOP) obtained from the original Multi-Objective one, but skips redundant resolutions by exploiting information from the current SOP.

AUGMECON-R was implemented with Python 3.8.10 as programming language, while the SOPs were solved with ILOG CPLEX® version 20.1 solver. The experiments were run on a server equipped with two Intel Xeon Gold 6246 R 3.4ghz CPUs, 512GB Ram and Ubuntu Server 20.04. LTS.

Section 3.1 describes the dataset used in the experiments and Section 3.2 details the definition of the SOP and the tuning of AUGMECON-R parameters. The numerical results are analysed in Section 3.3.

3.1. Benchmark instances `SH81`

The experiments were conducted on a set of 81 benchmark instances, namely `SH81`, which are based on real data provided by the WM Team at Sheffield City Council in South Yorkshire (UK). Indeed, from the analysis of historical data relating to the running costs, management and use of Sheffield's operating HWRCs, we have derived the parameters values as detailed below.

The SH81 instances were obtained from the Geographical Information System data of the Sheffield area. Population data refer to the Census (Office for National Statistics, 2011), according to which there were 229922 households in Sheffield, aggregated in 1744 cells (Barisone et al., 2019), as shown in Figure 1. The geographical coordinates of the centroids of each cell were provided by the WM team.

With regard to the candidate HWRCs, the WM Team has provided a confidential list of 9 alternative sites for the centres, the purpose of which is to enable us to define a realistic benchmark and explore the potential of the model being developed. In other words, these sites do not represent the actual locations that would be considered for a possible reconfiguration of the HWRCs network. In fact, these experiments are exploratory in nature. They provide a compelling demonstration of the tool's potential to offer tangible support for decision-making processes.

We obtained three classes of instances, *small*, *medium*, and *large*, either by considering all 1744 cells (in "large") or by randomly selecting 25% (i.e., 436 for the "small") and 50% (i.e., 872 for the "medium") of the available cells. Then, for each number of cells, we considered a total of 5, 7 or 9 sites chosen from the list provided. Functions and parameters (see Table 1) were set up as follows, assuming that the HWRCs operated seven days a week, with eight-hour shifts per day.

Capacity. This function is estimated from the data on affluence to Sheffield's active centres, considering the maximum number of users visiting the site per time slots of 15 min, and assuming that the centres were always working at full speed. The analysis of these data highlighted that the *hourly user rate* (*hur*) of each site linearly depends on the corresponding number of parking slots, which in turn linearly depends on the dimension of the site.

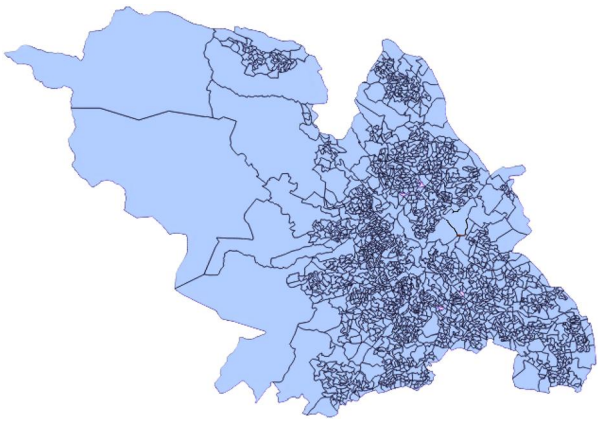

Figure 1. Map showing the distribution of cells for the city of Sheffield, in South Yorkshire (UK).

Running cost. This function is given by the sum of three different cost functions, estimated from historical data, related to the centre's labour and maintenance operations, namely: *Labour costs* ($\mathcal{L}$), *Asset costs* ($\mathcal{A}$), and *Overhead costs* ($\mathcal{O}$). Values are expressed in tens of thousands of pounds, namely: $r = (\mathcal{L} + \mathcal{A} + \mathcal{O})/10000$.

Demand. For each cell $i \in I$ the corresponding demand value was assumed to be equal to the number of users aggregated in the cell.

Distance. Euclidean distance was used as the distance function and distance values are expressed in hundreds of metres.

P. The maximum number of allowed facilities was left vary in the set $\{2, 3, 4\}$.

D. Given the maximum distance between a cell and a facility site, i.e., D_{MAX}, the threshold distance was left to vary in the set of rounded values $\{D_{\text{MAX}}/8, D_{\text{MAX}}/4, D_{\text{MAX}}/2\}$ for each instance.

Table 2 shows the number of cells and sites and the corresponding sets of values for the *D* and *P* parameters for this benchmark. Overall, the threshold distance ranges between 21 and 131 (i.e., 2100 and 13,100 m). Indeed, the set of *D* values provides a sufficiently diverse representative sample to allow extrapolation of generalizable results, given that the diameter of the smallest circle enclosing Sheffield is 17,899 m.

3.2. Calibration of parameters

When defining the SOP to be solved at each iteration of the AUGMECON framework, the prioritisation rule chosen for the objective functions does not affect the Pareto Set obtained. However, it could lead to the exploration of a less wide grid for the ε parameters, thus speeding up the computation (Mavrotas, 2009). For this purpose, we considered the average ranges for $\mathcal{RC}$, $\mathcal{UC}$ and $\mathcal{CO}$ on the whole dataset, computing these ranges from the payoff tables obtained with the lexicographic built-in function of the library IBM® Decision Optimization CPLEX® Modeling for Python. We then assigned the highest priority to $\mathcal{UC}$, that has the maximum

Table 2. Parameter values for the additional set of benchmark instances.

Inst. type	Cells	Sites	*D*	*P*
small	436	5	{21, 42, 84}	{2, 3, 4}
		7	{23, 46, 91}	
		9	{23, 47, 94}	
medium	872	5	{21, 42, 84}	{2, 3, 4}
		7	{23, 46, 91}	
		9	{27, 54, 108}	
large	1744	5	{25, 51, 102}	{2, 3, 4}
		7	{28, 55, 110}	
		9	{33, 66, 131}	

average range, and the lowest priority to $\mathcal{CO}$ that has the minimum average range.

In addition, we calibrated the parameter δ featured in the objective function of the SOP by testing AUGMECON-R on a sample set consisting of 20 SH81 instances ($\approx 25\%$ of the dataset), chosen randomly but with one representative for almost every possible configuration of $|I| + |J|$ and P. The grid of ε values was obtained with unitary discretisation step, while δ varied in the set $\{10^{-6}, 10^{-5}, 10^{-4}, 10^{-3}\}$, as suggested in Mavrotas and Florios (2013). We chose $\delta = 10^{-5}$ as it minimises the average CPU time gap, i.e., the average of the difference, for each instance, between the CPU time used by the algorithm and the minimum CPU time needed to solve this instance.

3.3. Numerical results

The results of the experiments conducted on the SH81 instances are presented in Table 3 which reports the number of Cells and the value of P. For each number of sites, the table also provides the value of D, the CPU time required by the AUGMECON-R method in seconds (column "CPU"), the number of efficient solutions (column "Sol."), of single objective problems solved by the method (column "#SOPs"), and the CPU time taken by CPLEX to solve an SOP.

These data show that for the *small* and *medium* instances across all maximum numbers of sites available (i.e., 5, 7, or 9) and threshold values D, as the value of P increases, the average CPU time of AUGMECON-R also increases. In fact, such a result is related to the higher average number of SOPs solved. Furthermore, it is worth noting that the trends in the average CPU times of CPLEX for solving an SOP depend on the fact that the number of binary variables and linear constraints of HWRC-Loc grows linearly with $|I|$ and $|J|$, as observed in Section 2.2. In fact, for any fixed number of sites $|J|$, D value in $\{D_{\text{MAX}}/2, D_{\text{MAX}}/4, D_{\text{MAX}}/8\}$ and P value, the CPU times increase as the number of cells increases. Similarly, for any fixed number of cells, D and P, the corresponding CPU times increase as the number of available sites increases, with the sole exception of the *large* instances with $|J| = 9$. The analysis of the CPU time of AUGMECON-R highlights also that for the *small* instances, for any fixed $|J|$ and P, as the threshold distance decreases the problem becomes harder to solve. There is no similar trend for *medium* and *large* instances, whose complexity varies according to the combination of $|J|$, P and D parameters.

Figure 2 depicts the trends for the average number of Pareto optimal solutions with respect to the threshold distance: for each Instance Type, we observe how by fixing one parameter in turn between $|J|$ and P and letting the other vary, more efficient solutions are obtained on average; in particular this appears by looking at the yellow columns in the figure as $|J|$ increases.

In fact, as there is a greater number of facilities to locate, there are potentially more feasible network configurations. Furthermore, for any fixed value of P, the largest average number of efficient solutions is obtained on the *small* instances for any possible

Table 3. Numerical results on the SH81 instances. CPU times in seconds and threshold distances in hundreds of metres.

Cells	P	$\|J\| = 5$					$\|J\| = 7$					$\|J\| = 9$				
		D	CPU	Sol.	#SOPs	CPU/ #SOPs	D	CPU	Sol.	#SOPs	CPU/ #SOPs	D	CPU	Sol.	#SOPs	CPU/#SOPs
436	2	84	12.28	3	67	0.18	91	34.80	5	249	0.14	94	742.91	8	2058	0.36
436	2	42	30.21	3	338	0.09	46	104.60	5	760	0.14	47	765.89	9	2499	0.31
436	2	21	42.94	3	995	0.04	23	1141.44	6	3619	0.32	23	6541.05	10	11097	0.59
436	3	84	71.96	6	662	0.11	91	47.30	7	313	0.15	94	879.60	12	3066	0.29
436	3	42	163.63	6	1392	0.12	46	147.40	7	1002	0.15	47	1011.83	13	3379	0.30
436	3	21	455.39	6	4279	0.11	23	1287.01	7	5029	0.26	23	6227.95	11	10040	0.62
436	4	84	76.52	8	729	0.10	91	226.82	11	908	0.25	94	6738.69	16	16204	0.42
436	4	42	203.57	8	1765	0.12	46	445.14	11	2021	0.22	47	1511.99	17	4456	0.34
436	4	21	567.09	8	5829	0.10	23	3378.35	11	11754	0.29	23	8452.03	15	15528	0.54
872	2	84	0.22	1	1	0.22	91	185.68	3	768	0.24	108	1472.47	4	2003	0.74
872	2	42	0.34	1	1	0.34	46	1362.07	4	1567	0.87	54	2929.75	5	2552	1.15
872	2	21	0.27	1	1	0.27	23	239.02	2	673	0.36	27	340.27	3	726	0.47
872	3	84	70.42	4	596	0.12	91	203.66	5	849	0.24	108	1938.94	7	2272	0.85
872	3	42	262.03	4	1391	0.19	46	2233.86	9	3528	0.63	54	6333.02	12	5095	1.24
872	3	21	280.60	4	1636	0.17	23	836.21	4	1692	0.49	27	5189.86	7	3441	1.51
872	4	84	71.53	6	663	0.11	91	612.08	9	1504	0.41	108	3245.43	11	2916	1.11
872	4	42	313.44	6	1636	0.19	46	2826.30	14	4155	0.68	54	6207.55	16	5457	1.14
872	4	21	319.36	6	2164	0.15	23	4196.12	8	6749	0.62	27	13313.79	13	10781	1.23
1744	2	102	1445.88	2	596	2.43	110	89602.07	6	19676	4.55	131	14322.80	6	3155	4.54
1744	2	51	3843.38	2	1290	2.98	55	2659198.37	5	669884	3.97	66	132888.28	6	22955	5.79
1744	2	25	3451.06	2	1328	2.60	28	176106.26	5	49523	3.56	33	95553.31	5	19391	4.93
1744	3	102	1011.54	2	596	1.70	110	23465.80	6	5638	4.16	131	18809.40	10	5051	3.72
1744	3	51	2025.37	2	1290	1.57	55	1190394.46	6	348249	3.42	66	390623.79	8	33671	11.60
1744	3	25	1962.18	2	1328	1.48	28	54589.56	5	12712	4.29	33	208715.91	7	23733	8.79
1744	4	102	984.41	2	596	1.65	110	24198.59	7	6567	3.68	131	15726.43	9	5334	2.95
1744	4	51	1823.05	2	1290	1.41	55	1190438.06	9	354704	3.36	66	195147.88	9	40291	4.84
1744	4	25	1698.10	2	1328	1.28	28	40078.85	6	16857	2.38	33	171638.74	9	32193	5.33

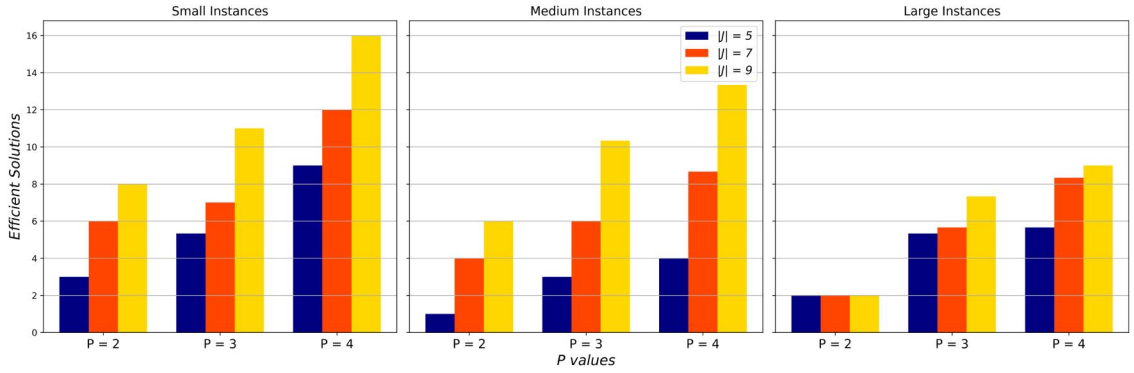

Figure 2. Trends in average number of efficient solutions for each Instance Type and with respect to the threshold distance. Values grouped by the maximum number of sites available (i.e., $|J|$); columns in a group report data for each number of sites available.

Table 4. Average values for each objective function. $\mathcal{RC}$ values expressed in tens of thousands of pounds; $\mathcal{CO}$ and $\mathcal{UC}$ values scaled by dividing by 50.

Cells	P	$\|J\| = 5$					$\|J\| = 7$					$\|J\| = 9$				
		D	Sol.	avg($\mathcal{UC}$)	avg($\mathcal{RC}$)	avg($\mathcal{CO}$)	D	Sol.	avg($\mathcal{UC}$)	avg($\mathcal{RC}$)	avg($\mathcal{CO}$)	D	Sol.	avg($\mathcal{UC}$)	avg($\mathcal{RC}$)	avg($\mathcal{CO}$)
436	2	84	3	98345.00	86.67	2322.00	91	5	90256.20	176.40	2322.00	94	8	81642.00	355.38	2424.38
436	2	42	3	99334.00	87.00	2162.33	46	5	90256.20	176.40	2267.40	47	9	80424.56	381.89	2385.78
436	2	21	3	98345.00	86.67	800.33	23	6	88016.00	249.00	1307.50	23	10	80063.60	404.90	1231.50
436	3	84	6	91103.17	279.67	2322.00	91	7	86671.71	207.86	2322.00	94	12	74962.67	414.83	2435.75
436	3	42	6	91597.67	279.83	2204.67	46	7	86671.71	207.86	2278.57	47	13	74633.62	428.62	2412.38
436	3	21	6	91103.17	279.67	1037.17	23	7	86671.71	207.86	1356.14	23	11	75359.36	398.73	1439.00
436	4	84	8	89015.88	379.12	2322.00	91	11	79606.00	384.09	2322.00	94	16	70683.06	479.00	2441.44
436	4	42	8	89386.75	379.25	2215.25	46	11	79606.00	384.09	2294.36	47	17	70683.18	485.76	2422.94
436	4	21	8	89015.88	379.12	1107.25	23	11	79606.00	384.09	1630.55	23	15	70525.27	481.27	1669.87
872	2	84	1	177382.00	130.00	4788.00	91	2	181801.00	228.67	4813.00	108	4	211192.00	363.00	4894.25
872	2	42	1	177382.00	130.00	4007.00	46	4	167451.50	341.25	4422.75	54	5	166759.60	441.20	4679.60
872	2	21	1	177382.00	130.00	1493.00	23	2	170477.50	220.00	1962.00	27	3	168447.33	251.00	2517.00
872	3	84	4	174078.25	387.00	4788.00	91	5	173980.00	251.80	4812.00	108	7	163814.86	393.57	4902.86
872	3	42	4	174078.25	387.00	4057.00	46	9	159987.67	426.00	4487.78	54	12	151165.17	591.58	4800.08
872	3	21	4	174078.25	387.00	1604.25	23	4	166363.00	253.25	2105.75	27	7	158091.86	403.14	2649.86
872	4	84	6	173127.50	483.83	4788.00	91	9	160740.00	447.67	4814.67	108	11	154439.82	494.64	4924.55
872	4	42	6	173127.50	483.83	4070.00	46	14	155086.86	515.64	4530.79	54	16	146534.75	578.69	4808.25
872	4	21	6	173127.50	483.83	1633.00	23	8	155276.50	472.88	2439.25	27	13	148962.85	545.46	2881.31
1744	2	102	2	569199.50	663.50	9827.00	110	6	559283.33	464.50	9861.50	131	6	547626.00	532.50	10187.67
1744	2	51	2	569199.50	663.50	5214.50	55	5	556497.00	484.20	6051.00	66	6	559283.33	464.50	7110.00
1744	2	25	2	569199.50	663.50	1040.50	28	5	556497.00	484.20	2052.60	33	5	556497.00	484.20	2907.60
1744	2	102	3	569199.50	663.50	9827.00	110	6	541792.67	468.00	9861.50	131	10	498202.30	769.70	10229.00
1744	2	51	3	569199.50	663.50	5214.50	55	6	521804.17	498.83	6551.17	66	8	514183.88	664.62	7649.38
1744	2	25	3	569199.50	663.50	1040.50	28	5	535508.20	488.40	2457.80	33	7	505750.86	707.29	3556.57
1744	2	102	4	569199.50	663.50	9827.00	110	7	520503.43	483.29	9889.57	131	9	485495.11	706.89	10222.11
1744	2	51	4	569199.50	663.50	5214.50	55	9	486782.89	605.67	6977.56	66	9	493266.67	661.56	7874.89
1744	2	25	4	569199.50	663.50	1040.50	28	6	511718.17	502.83	2793.00	33	9	475976.44	728.78	4012.67

value of $|J|$. This is because, when the number of cells is limited, there are potentially several feasible configurations for the allocation of demand nodes that satisfy, in particular, the capacity constraints (1d).

Finally, we analyse the extent to which the values of the objective functions are affected by the number of cells, sites, threshold distance and allowed facilities. Table 4 reports the average values for $\mathcal{UC}$, $\mathcal{RC}$ and $\mathcal{CO}$: for each instance, we calculated the average of the values that each function takes in the efficient solutions found.

First, we observe that for fixed numbers of cells and sites and fixed threshold distance D, the average values of $\mathcal{UC}$ decrease as P increases. This result is based on the fact that by increasing the maximum number of facilities to locate, potentially more demand nodes can be assigned to closer active facilities, leading to improved user satisfaction with the service provided. Naturally, the *large* instances are those characterised by the highest average values of $\mathcal{UC}$, as they contain more demand nodes. Conversely, the average values of $\mathcal{RC}$ naturally increase with P, as more facilities can be located. In addition, for the same $|J|$ and P, the highest values of $\mathcal{RC}$ are related to *large* instances, meaning that potentially more expensive facilities are needed to ensure a certain level of user satisfaction. Similarly, for any fixed number of cells and sites and fixed D, the average values of $\mathcal{CO}$ increase as P increases. This is due to the fact that an increased number of active centres leads to improved coverage for the service demand. For example, Figure 3 plots the average

percentage of covered demand corresponding to the lowest threshold, namely $D = D_{MAX}/8$, aggregating data with respect to $|J|$.

The information derived from this representation is twofold: on the one hand, it highlights that the reduction of the coverage radius has a stronger effect on those instances characterised by a larger number of demand nodes, as the *large* instances have the lowest average percentage of demand covered. On the other hand, it highlights that the instances characterised by larger values of P have, on average, better values of $\mathcal{CO}$ (cf. the yellow columns). However, the coverage is affected by the threshold distance, as can be seen from the trends of the objective function values. In fact, for any fixed number of cells and sites, and any fixed P, the values of $\mathcal{CO}$ decrease with D. In particular, Figure 4 shows the trends for the average $\mathcal{CO}$ value, aggregated by P.

For each Instance Type, as expected the (average) coverage values increase with increasing D, meaning that less tight threshold distances lead to improved demand coverage. Moreover, for any fixed D, the highest (average) $\mathcal{CO}$ values are associated with instances with $|J| = 9$, as shown by the data for *medium* and *large* instances. In conclusion, as expected, the values of the coverage function $\mathcal{CO}$ depend on the coverage radius, being better for higher radii. Moreover, this analysis allowed to observe that the different values of the parameter D also have an impact on the computational level, eventually leading to more complex problems.

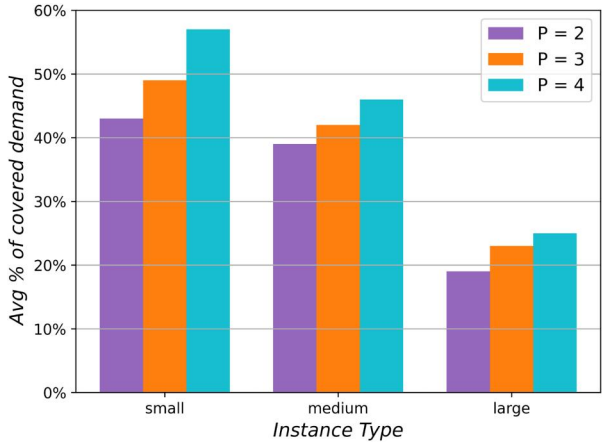

Figure 3. Trends in average percentage of demand covered for each Instance Type. Data refer to instances with $D = D_{MAX}/8$ and are aggregated by the value of $|J|$, i.e., the number of facilities available for installation.

4. A soft-constrained version of the household waste recycling centres location problem

It is fairly frequent in the scientific literature to find versions of classical problems in which the violation of one or more classes of constraints is allowed. In general, this approach has a dual purpose: to allow a more realistic representation of specific scenarios in which the problem arises, and to explore the computational impact that these constraints have on the method used to solve the problem.

Specifically, in the related literature on Capacitated Facility Location problems, the capacity constraints are often treated as *soft constraints* (Estrada-Moreno et al., 2020; Han et al., 2020). In fact, it may be possible to violate them while taking into account ad hoc defined *penalty costs* in the objective function(s) since, depending on the specific problem setting, it may be preferable to have a small number of congested facilities when capacity is exceeded to a limited extent. It should be emphasised that, although the soft constraints allow exploration of an extended feasible region, the primary purpose of the penalty costs is to discourage excessive deviation from that region.

Following this strategy, we defined a soft-constrained version of the HWRC-Loc in which the capacity constraints (1d) can be violated when allocating demands, but an excessive deviation is discouraged by the penalty costs added to $\mathcal{RC}$ and $\mathcal{UC}$. In particular, although these costs are a mathematical tool to ensure that the search for efficient solutions takes place in a neighbourhood of the initial set of alternatives, we can associate a managerial counterpart to them. In fact, if the capacity of at least one facility is exceeded, additional labour will be required to run that facility efficiently, thus affecting $\mathcal{RC}$. Similarly, relaxing the capacity

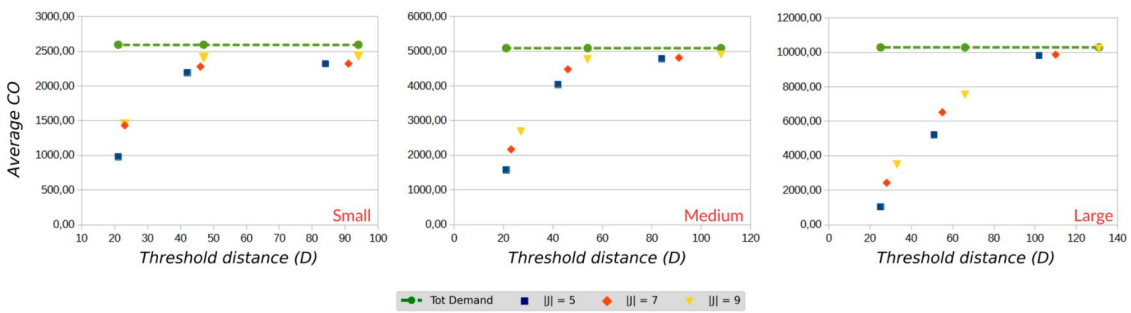

Figure 4. Trends in average $\mathcal{CO}$ function for each Instance Type. Data aggregated (in each plot) by the value of the parameter P.

constraints would strongly influence the assignment of users to active facilities, thus improving the perceived quality of service. However, this would inevitably lead to the exploration of unrealistic configurations if users were not penalised for being assigned to congested facilities in the $\mathcal{UC}$ function.

Section 4.1 details a Mixed Integer Linear Programming formulation for our soft-constrained approach to the HWRC-Loc.

4.1. A mixed integer linear programming model

The violation of soft constraints is usually formulated using *piecewise linear functions* (Archetti et al., 2021; Estrada-Moreno et al., 2020); to this end, for each facility site $j \in J$ we introduced the variable τ_j defined as the percentage of its capacity that is exceeded by the total demand allocated to that site (cf. (6)).

$$\tau_j = \max\left\{\frac{\sum_{i\in I} h_i y_{ij} - c_j}{c_j}, 0\right\}. \tag{6}$$

The penalty costs added to $\mathcal{RC}$ represent the percentage of additional running costs associated with overloaded facilities and are defined by (7). The term $(1-\lambda_{\mathcal{RC}})$ represents a *tolerance* factor to calibrate and related to the violation of capacity constraints.

$$PC_{\mathcal{RC}} = (1-\lambda_{\mathcal{RC}}) \sum_{j\in J} r_j \tau_j \tag{7}$$

Given the user costs associated with a facility $j \in J$, i.e., $\mathcal{UC}_j = \sum_{i\in I} h_i d_{ij} y_{ij}$, that denotes the cost of the demand assigned to j, we extend it by including a penalty related to the congestion of that facility:

$$\mathcal{UC}^*_j := \begin{cases} \mathcal{UC}_j & \text{if } \tau_j = 0, \\ \sum_{i\in I} h_i d_{ij}\left[1 + (1-\lambda_{\mathcal{UC}}) c_j \tau_j\right] y_{ij} & \text{otherwise.} \end{cases}$$

Thus, the penalty term of $\mathcal{UC}$ is given by (8) where the term $(1-\lambda_{\mathcal{UC}})$ represents the tolerance factor, as in (7):

$$PC_{\mathcal{UC}} = (1-\lambda_{\mathcal{UC}}) \sum_{i\in I} \sum_{j\in J} h_i d_{ij} c_j \tau_j y_{ij}. \tag{8}$$

Indeed, $PC_{\mathcal{UC}}$ is a quadratic function since the terms $\tau_j y_{ij}$ are the product between a continuous variable (τ_j) and a binary variable (y_{ij}). However it can be linearised with a well-established procedure from the literature which consists in introducing the continuous variables k_{ij} defined to represent each product, and the constraints (9) $\forall i \in I, \forall j \in J$, in which the parameter $M_j := (\sum_{i\in I} h_i - c_j)/c_j$ is an upper bound for τ_j $\forall j \in J$ (Asghari et al., 2022).

$$k_{ij} \geq 0 \quad \text{and} \quad k_{ij} \leq M_j \quad \text{and} \quad k_{ij} \leq \tau_j \quad \text{and} \quad \tau_j - k_{ij} \leq M_j(1-y_{ij}) \tag{9}$$

Therefore, the penalty costs can be reformulated with the k variables as:

$$PC'_{\mathcal{UC}} = (1-\lambda_{\mathcal{UC}}) \sum_{i\in I} \sum_{j\in J} h_i d_{ij} c_j k_{ij}.$$

The resulting Multi-Objective Mixed Integer Linear Program is given by (10) where (10a) minimises the sum of the running costs and the corresponding penalty costs; (10b) minimises the user costs and the corresponding penalty costs.

$$\begin{aligned}
&(\text{HWRC-Loc}_{soft}) \min\ (\mathcal{RC} + PC_{\mathcal{RC}}) && \text{(10a)}\\
&\qquad\qquad \min\ (\mathcal{UC} + PC'_{\mathcal{UC}}) && \text{(10b)}\\
&\qquad\qquad \max\ \mathcal{CO} && \text{(10c)}\\
&\text{subject to} \\
&\text{Constraints (1e)-(1f), (1h)-(1i), (2)} && \text{(10d)}\\
&k_{ij} \leq M_j && \forall i \in I, \forall j \in J \quad \text{(10e)}\\
&k_{ij} \leq \tau_j && \forall i \in I, \forall j \in J \quad \text{(10f)}\\
&\tau_j - k_{ij} \leq M_j(1-y_{ij}) && \forall i \in I, \forall j \in J \quad \text{(10g)}\\
&\tau_j \geq \frac{\sum_{i\in I} h_i y_{ij} - c_j}{c_j} && \forall j \in J \quad \text{(10h)}\\
&\tau_j \geq 0 && \forall j \in J \quad \text{(10i)}\\
&k_{ij} \geq 0 && \forall i \in I, \forall j \in J \quad \text{(10j)}
\end{aligned}$$

The resulting model encompasses: $|I| + |J| + |I||J|$ binary variables, $|J| + |I||J|$ continuous variables, and $5|I||J| + 3|I| + 4|J| + 1$ linear constraints.

It is worth mentioning that since we have relaxed the constraints (1d), there may be efficient solutions that violate the activation constraints. Therefore, when computing the "soft" Pareto Sets, we restore the feasibility for this kind of solutions.

4.2. Computational experiments

For the purposes of comparing the initial and soft approaches to HWRC-Loc, we modified the benchmark of instances described in Section 3.1 to make the capacity constraints tighter by multiplying the capacities by 0.6. This change was made in order to better assess the effects of relaxing these constraints.

The experiments were conducted by running AUGMECON-R with the same setting detailed in Section 3.2. Additionally, to allow a computational comparison between the approaches as fair as possible, we have used the number of grid-points explored by AUGMECON-R in the "non soft" case as a proxy to obtain the grid for the ε values when the ranges of the $\mathcal{RC}$ and $\mathcal{CO}$ functions are wider.

Finally, we let the λ values vary in the set $\{-1, 0, 0.5\}$ to explore different scenarios, as these parameters define the extent to which the violation of capacity constraints is acceptable. Specifically, $\lambda = -1$ means a "low" tolerance to violation, so the

penalty costs are weighted twice in the corresponding objective function; with $\lambda = 0$ the tolerance is "medium", while with $\lambda = 0.5$ it is "high", since only half of the penalty costs are added to the objective function. The experiments featured five pairs of $(\lambda_{\mathcal{RC}}, \lambda_{\mathcal{UC}})$ values: $(-1, -1)$, $(-1, 0)$, $(0, -1)$, $(0, 0)$, and $(0.5, 0.5)$.

4.2.1. Computational analysis of numerical results

The analysis in this section focuses on CPU times, number of SOPs solved and of efficient solutions. Specifically, the comparison in terms of CPU times and number of SOPs solved, reported in Table 5, is based on experimental data aggregated with respect to the parameter P as similar trends were observed for values ranging from 2 to 4. Accordingly, the groups of instances are denoted as "Cells_Sites_D". For each group, the table reports the average CPU times and the average number of SOPs solved during AUGMECON-R iterations (avg(#SOPs)) both for the original problem ("non soft") and for each configuration of the tolerance values. The last column reports the maximum average CPU time.

These data show that, with the sole exception of the *small* instances with 5 candidates and $D = D_{\text{MAX}}/4$, the maximum average CPU times are obtained by solving the original HWRC-Loc (cf. values in bold). In particular, this result is not only influenced by the fact the soft-constrained approach solves on average the 12% of the number of SOPs solved with the hard-constrained approach. In fact, a deeper analysis of the average CPU time needed to solve an SOP shows that the resolution of SOPs is faster in the "soft" configurations, with the sole exception of the *small* instances with $|J| = 5$. Specifically, on average the CPU time required to solve an SOP in the soft cases is 50% of the CPU time required in the non-soft case, with a minimum of 21.84% and a maximum of 93.97%, respectively for the *large* instances with $|J| = 5$ and $\lambda_{\mathcal{RC}} = \lambda_{\mathcal{UC}} = 0$ and the *medium* ones with $|J| = 5$ and $\lambda_{\mathcal{RC}} = \lambda_{\mathcal{UC}} = 0.5$. This proves that the introduction of soft constraints is beneficial from a computational standpoint, since it leads to a significant reduction in the average CPU time needed to solve a problem instance. Furthermore, we observed that soft configurations characterised by the same number of solved SOPs exhibit similar average CPU times. This suggests that tolerance value parameters have no impact on problem complexity.

As was previously noted for the original HWRC-Loc, the trend in the average CPU times for CPLEX to solve an SOP for the soft-constrained problem is also consistent with the linear dependence of the number of variables and constraints on the number of cells and sites. Moreover, even with the soft-constrained approach, it emerges that as the coverage radius D decreases, the problem becomes more complex. Finally, comparing the CPU time required to solve a hard-constrained SOP for the benchmark instances

Table 5. Aggregated numerical results with respect to the parameter P. Maximum average CPU for each group of instances in the last column and evidenced in bold in the corresponding rows.

	Average												Maximum avg. CPU
	non-soft		$\lambda_{\mathcal{RC}}=0$ $\lambda_{\mathcal{UC}}=0$		$\lambda_{\mathcal{RC}}=0$ $\lambda_{\mathcal{UC}}=-1$		$\lambda_{\mathcal{RC}}=-1$ $\lambda_{\mathcal{UC}}=0$		$\lambda_{\mathcal{RC}}=-1$ $\lambda_{\mathcal{UC}}=-1$		$\lambda_{\mathcal{RC}}=0.5$ $\lambda_{\mathcal{UC}}=0.5$		
Cells_Sites_D	CPU	#SOPs	CPU	#SOPs	CPU	#SOPs	CPU	#SOPs	CPU	#SOPs	CPU	#SOPs	
436_5_$D_{\text{MAX}}/8$	**66.95**	1270.33	23.31	141.67	23.24	140.67	23.62	135.33	23.65	135.33	25.21	151.00	66.95
436_5_$D_{\text{MAX}}/4$	6.58	420.00	9.81	57.00	9.72	57.00	8.76	57.67	8.67	58.00	**12.63**	71.67	12.63
436_5_$D_{\text{MAX}}/2$	**47.96**	420.00	5.87	49.00	5.87	49.00	5.87	49.00	5.83	49.00	6.29	49.00	47.96
872_5_$D_{\text{MAX}}/8$	**511.55**	1439.67	48.98	147.67	49.28	147.67	46.08	138.33	46.52	138.33	69.94	189.67	511.55
872_5_$D_{\text{MAX}}/4$	**535.59**	1281.00	56.58	163.00	56.46	163.00	51.17	141.00	50.61	141.00	73.66	189.67	535.59
872_5_$D_{\text{MAX}}/2$	**150.50**	573.67	15.97	69.00	16.05	69.00	16.42	69.00	17.13	69.00	17.42	69.00	150.50
1744_5_$D_{\text{MAX}}/8$	**2373.20**	994.00	71.92	129.00	72.55	119.33	82.63	158.33	77.56	149.00	77.41	121.67	2373.20
1744_5_$D_{\text{MAX}}/4$	**4686.17**	1752.00	91.29	147.67	101.47	171.00	83.59	134.00	87.92	142.33	102.43	150.00	4686.17
1744_5_$D_{\text{MAX}}/2$	**2423.49**	857.00	53.57	89.33	55.02	92.67	52.08	86.00	52.16	84.67	57.97	91.00	2423.49
436_7_$D_{\text{MAX}}/8$	**833.24**	3276.00	47.91	318.00	60.02	430.33	52.43	338.33	49.31	323.00	46.05	322.67	833.24
436_7_$D_{\text{MAX}}/4$	**127.97**	699.00	15.85	104.00	14.73	98.33	19.54	135.67	19.02	135.67	15.50	105.67	127.97
436_7_$D_{\text{MAX}}/2$	**108.95**	424.00	6.32	57.00	6.14	57.00	6.04	57.00	6.25	57.00	6.32	57.00	108.95
872_7_$D_{\text{MAX}}/8$	**18546.20**	17834.33	167.39	484.33	174.91	483.33	168.83	485.67	157.85	467.33	185.54	543.00	18546.20
872_7_$D_{\text{MAX}}/4$	**36857.91**	34186.67	130.00	394.00	128.80	385.67	192.17	574.33	187.05	565.33	142.11	408.33	36857.91
872_7_$D_{\text{MAX}}/2$	**4889.16**	5168.00	53.46	192.33	55.78	202.67	49.50	235.67	49.27	231.33	51.07	170.00	4889.16
1744_7_$D_{\text{MAX}}/8$	**30202.35**	7991.33	1638.74	464.33	1588.94	442.67	1203.09	408.67	1253.14	412.00	1592.88	476.00	30202.35
1744_7_$D_{\text{MAX}}/4$	**38584.36**	9581.67	2438.95	594.67	2711.42	655.33	1104.57	384.00	1095.68	381.33	2679.66	715.33	38584.36
1744_7_$D_{\text{MAX}}/2$	**3153.29**	970.33	212.27	89.00	216.56	89.00	148.11	89.00	149.04	89.00	227.38	89.00	3153.29
436_9_$D_{\text{MAX}}/8$	**2476.86**	4789.00	83.66	500.67	65.03	394.00	75.97	474.67	76.64	452.67	66.59	454.33	2476.86
436_9_$D_{\text{MAX}}/4$	**827.18**	2794.33	30.90	182.33	29.79	182.33	28.57	181.67	30.40	181.67	27.26	182.67	827.18
436_9_$D_{\text{MAX}}/2$	**2907.13**	6977.33	50.08	383.67	40.68	330.67	38.21	330.67	41.60	336.33	35.62	330.67	2907.13
872_9_$D_{\text{MAX}}/8$	**6247.25**	5173.33	120.13	310.00	125.75	349.67	106.37	338.00	113.08	336.33	175.41	514.00	6247.25
872_9_$D_{\text{MAX}}/4$	**34737.59**	32213.33	245.59	809.00	231.74	785.33	235.50	829.33	285.81	928.00	175.11	558.00	34737.59
872_9_$D_{\text{MAX}}/2$	**4379.51**	3911.00	60.47	207.33	59.51	207.33	52.48	207.33	55.65	207.33	49.53	186.00	4379.51
1744_9_$D_{\text{MAX}}/8$	**358551.06**	35344.67	4851.98	1356.00	4469.28	1305.00	2665.79	892.33	2700.19	889.67	3726.09	1092.33	358551.06
1744_9_$D_{\text{MAX}}/4$	**320862.75**	50191.67	8393.03	1767.00	10867.27	2260.33	6099.31	1186.33	6085.94	1188.00	9561.24	1980.00	320862.75
1744_9_$D_{\text{MAX}}/2$	**201591.28**	34986.00	1406.99	443.00	1421.57	447.67	1317.31	538.33	1437.83	538.33	1330.78	446.00	201591.28

(cf. Table 3) and an SOP for these instances characterised by reduced capacities, highlights that tightening the capacity constraints poses significant challenges to solving the HWRC-Loc. On average 30% more CPU time is required to solve an SOP with reduced capacities, with some instances requiring up to 94.84% more CPU time. These results demonstrate the particular benefit of the soft-constrained approach to the HWRC-Loc in real-world scenarios involving stringent coverage radius requirements and sites with reduced service capacities.

To compare the number of efficient solutions obtained with the non-soft approach and with each pair of tolerance values, we aggregated the experimental data with respect to the parameter D in Table 6.

As expected, the configurations with soft constraints are characterised by a higher average number of efficient solutions with the exception of the *large* instances with $P = 2$. In fact, these constraints allow to explore a larger region in the search for efficient solutions. Nevertheless, the hard-constrained approach produces more efficient alternatives for the *large* instances when the minimum number of facilities has to be located, suggesting that the complexity of the HWRC-Loc also depends on other classes of constraints, with the CACs likely to be hard to satisfy even if the capacity requirements are relaxed. However, the soft-constrained approach produces on average 1.5 times as many efficient solutions as the non-soft configuration of the HWRC-Loc, with this number doubling for the *medium* instances.

Focusing on the soft configurations, we observed that for any Instance Type and P value, the average number of efficient solutions increases with $|J|$. This indicates that the inclusion of soft capacity constraints provides the decision-maker with a broader set of alternatives. Furthermore, for all the λ pairs, the *small* and *medium* instances exhibit the highest average number of efficient solutions. In particular, the Pareto Sets obtained with $\lambda_{\mathcal{RC}} = -1$ and $\lambda_{\mathcal{UC}} = 0$ and those with $\lambda_{\mathcal{RC}} = \lambda_{\mathcal{UC}} = 0.5$ are the most extensive. This suggests that when the tolerance for violating soft constraints is low for $\mathcal{RC}$ and medium for $\mathcal{UC}$, or high for both functions, a greater number of efficient alternatives can be provided for the design of the HWRCs network.

In conclusion, this analysis highlighted the valuable contribution of soft constraints in reducing the CPU time required to solve relaxed larger instances of HWRC-Loc, while also offering a broader range of alternatives to decision-makers through more extensive Pareto Sets.

4.2.2. Analysis of trends in objective functions values

This analysis is carried out by aggregating the averages of the objective functions values with respect to the parameter D. We observed that the soft-constrained approach with all the λ s pairs, except

Table 6. Aggregated average and max average number of efficient solutions for each group of instances. Data aggregated with respect to the parameter D. Maximum average number of solutions for each group of instances shown in the last column and evidenced in bold in the corresponding rows.

	avg(Sol.)						Maximum avg(Sol.)
Cells_Sites_P	non-soft	$\lambda_{\mathcal{RC}}=0$ $\lambda_{\mathcal{UC}}=0$	$\lambda_{\mathcal{RC}}=0$ $\lambda_{\mathcal{UC}}=-1$	$\lambda_{\mathcal{RC}}=-1$ $\lambda_{\mathcal{UC}}=0$	$\lambda_{\mathcal{RC}}=-1$ $\lambda_{\mathcal{UC}}=-1$	$\lambda_{\mathcal{RC}}=0.5$ $\lambda_{\mathcal{UC}}=0.5$	
436_5_2	1.00	**3.33**	**3.33**	**3.33**	**3.33**	**3.33**	3.33
436_5_3	4.00	6.00	**6.33**	**6.33**	**6.33**	**6.33**	6.33
436_5_4	6.00	**8.33**	8.00	**8.33**	**8.33**	**8.33**	8.33
872_5_2	2.00	**3.33**	**3.33**	**3.33**	**3.33**	**3.33**	3.33
872_5_3	3.00	**6.33**	**6.33**	**6.33**	**6.33**	6.00	6.33
872_5_4	5.00	**8.33**	**8.33**	**8.33**	**8.33**	**8.33**	8.33
1744_5_2	**2.00**	0.00	0.00	0.00	0.00	0.00	2.00
1744_5_3	2.00	**3.00**	**3.00**	**3.00**	**3.00**	2.33	3.00
1744_5_4	2.00	**5.00**	4.67	**5.00**	**5.00**	**5.00**	5.00
436_7_2	3.00	5.00	**5.33**	**5.33**	4.67	5.00	5.33
436_7_3	4.67	**7.67**	6.67	7.33	7.00	7.33	7.67
436_7_4	8.67	10.00	**10.67**	10.33	10.00	**10.67**	10.67
872_7_2	3.67	5.00	5.00	**5.33**	5.00	5.00	5.33
872_7_3	5.00	8.00	8.00	8.00	**8.33**	**8.33**	8.33
872_7_4	9.33	12.33	12.67	12.33	12.33	**13.00**	13.00
1744_7_2	**3.00**	1.33	1.33	1.00	1.00	1.00	3.00
1744_7_3	**5.00**	4.33	3.33	**5.00**	4.00	4.33	5.00
1744_7_4	6.67	**7.00**	6.00	6.00	6.33	6.33	7.00
436_9_2	5.67	6.33	6.00	6.00	5.33	**7.00**	7.00
436_9_3	9.33	10.33	10.00	10.67	10.67	**11.33**	11.33
436_9_4	13.67	13.67	13.33	**15.33**	12.67	14.00	15.33
872_9_2	4.67	5.33	5.67	5.00	**6.00**	**6.00**	6.00
872_9_3	7.67	11.00	11.67	11.33	**13.00**	11.67	13.00
872_9_4	12.00	16.00	**16.67**	15.00	15.00	15.67	16.67
1744_9_2	**4.33**	1.67	1.33	1.00	1.67	1.67	4.33
1744_9_3	**7.67**	4.67	5.00	6.00	4.67	6.33	7.67
1744_9_4	**10.00**	9.00	9.33	**10.00**	9.00	9.67	10.00

$(0,0)$, leads to improved $\mathcal{CO}$ values on the *large* instances, compared to the non-soft approach. In particular, the average improvement of the coverage values is 14% but it reaches the 30% on the instances with 9 candidates. Thus, when dealing with scenarios characterised by more demand nodes, exploring a neighbourhood of the initial feasible region could lead to configurations that better meet the coverage requirements. Additionally, compared to the average values of the non-soft case, those of $\mathcal{UC}$ are lower on the *large* instances with $|J| = 7, 9$, with $avg(\mathcal{UC})$ being $\approx 82\%$ of the corresponding non-soft averages, and the configurations with $\lambda_{\mathcal{RC}} = \lambda_{\mathcal{UC}} = 0.5$ and $\lambda_{\mathcal{RC}} = -1$ and $\lambda_{\mathcal{UC}} = 0$ lead to greater reductions of the objective function values.

To further investigate the effect on the $\mathcal{UC}$ function of relaxing the capacity constraints, we analyse the trade-off between the average user-site distance and the average violations. Specifically, for each instance, we averaged the user-site distances corresponding to the assignments in each solution, then aggregated these averages by D and did the same for the τ values. Table 7 reports these data for each pair of λ s; the $avg(\tau)$ are given in percentages, as τ_j denotes, for each site $j \in J$, the percentage of its capacity that is exceeded by the total demand allocated to that site.

The soft-constrained approach leads to the minimum average distance for *medium* instances with $P = 2$ and *large* instances. In particular, for any fixed value of $|J|$ these instances are characterised by the higher average violation of capacity constraints. This result further confirms that relaxing the capacity constraints is beneficial from the user's point of view for all scenarios characterised by more demand nodes, i.e., users, and/or fewer facilities available for installation. In addition, the analysis shows that the reduction in the distance between users and active facilities is more noticeable when comparing the hard and soft constrained approaches. On average, the hard configuration improves this distance by 11% over the soft configuration, while the soft configuration leads to an average improvement of 17.92%, with peaks of 38% for *large* instances. In conclusion, the exploration of the objective function values and the user-site distances trade-offs shows that, as the number of cells increases, user satisfaction can be improved by allowing the capacity constraints to be violated with more/less stringent tolerance thresholds.

Furthermore, by relaxing the capacity constraints, those network configurations that were unfeasible for the original HWRC-Loc, including the less operationally costly, become allowed, as evidenced by the reduction in running costs. In fact, the soft-constrained approach always leads to better $\mathcal{RC}$ values, with $avg(\mathcal{RC})$ being $\approx 62\%$ of the corresponding non-soft averages. In addition, on the *large* instances the improvements in the running

Table 7. Aggregated numerical results with respect to the parameter D. Minimum average of average distance for each group of instances in the last column and evidenced in bold in the corresponding rows.

	Average											Min average avg(dist.)
	non-soft	$\lambda_{\mathcal{RC}} = 0$ $\lambda_{\mathcal{UC}} = 0$		$\lambda_{\mathcal{RC}} = 0$ $\lambda_{\mathcal{UC}} = -1$		$\lambda_{\mathcal{RC}} = -1$ $\lambda_{\mathcal{UC}} = 0$		$\lambda_{\mathcal{RC}} = -1$ $\lambda_{\mathcal{UC}} = -1$		$\lambda_{\mathcal{RC}} = 0.5$ $\lambda_{\mathcal{UC}} = 0.5$		
Cells_Sites_*P*	avg(dist.)	avg(dist.)	avg(τ)	avg(dist.)	avg(τ)	avg(dist.)	avg(τ)	avg(dist.)	avg(τ)	avg(dist.)	avg(τ)	
436_5_2	**33.50**	38.23	1.23%	38.23	1.23%	38.23	1.23%	38.23	1.23%	38.23	1.23%	33.50
436_5_3	**32.78**	35.73	0.69%	35.53	0.65%	35.53	0.65%	35.53	0.65%	35.53	0.65%	32.78
436_5_4	**32.55**	34.71	0.49%	34.80	0.51%	34.71	0.49%	34.71	0.49%	34.71	0.49%	32.55
872_5_2	43.13	**39.59**	16.72%	**39.59**	16.72%	**39.59**	16.72%	**39.59**	16.72%	**39.59**	16.72%	39.59
872_5_3	**33.92**	36.90	8.78%	36.90	8.78%	36.90	8.78%	36.90	8.78%	37.07	9.35%	33.92
872_5_4	**33.79**	36.11	6.68%	36.11	6.68%	36.11	6.68%	36.11	6.68%	36.11	6.68%	33.79
1744_5_2	**57.04**	–	–	–	–	–	–	–	–	–	–	57.04
1744_5_3	57.04	**44.68**	34.38%	**44.68**	34.38%	**44.68**	34.38%	**44.68**	34.38%	44.75	34.49%	44.68
1744_5_4	57.04	**44.58**	33.83%	44.61	33.93%	**44.58**	33.83%	**44.58**	33.83%	**44.58**	33.83%	44.58
436_7_2	**31.02**	34.92	0.50%	34.58	0.50%	34.54	0.50%	35.32	0.59%	34.71	0.55%	31.02
436_7_3	**30.69**	33.32	0.40%	33.77	0.40%	33.19	0.36%	33.61	0.38%	33.19	0.37%	30.69
436_7_4	**28.47**	31.11	0.25%	30.93	0.25%	31.01	0.26%	31.07	0.27%	30.92	0.25%	28.47
872_7_2	43.02	37.57	8.03%	37.56	8.03%	**36.93**	7.63%	37.04	8.21%	37.56	8.03%	36.93
872_7_3	**31.81**	35.13	5.23%	34.96	5.23%	35.16	5.20%	34.74	5.10%	34.92	5.10%	31.81
872_7_4	**30.21**	32.48	3.29%	32.77	3.29%	32.91	3.55%	33.02	3.47%	32.87	3.20%	30.21
1744_7_2	50.18	45.32	15.01%	45.32	15.01%	**43.99**	16.21%	**43.99**	16.21%	**43.99**	16.21%	43.99
1744_7_3	47.66	43.57	17.94%	43.52	17.94%	43.47	14.52%	**43.39**	15.74%	43.94	17.17%	43.39
1744_7_4	46.54	42.61	13.39%	42.42	13.39%	42.69	13.34%	42.67	14.03%	**42.41**	12.88%	42.41
436_9_2	**28.50**	33.29	0.33%	33.29	0.37%	33.21	0.36%	33.85	0.44%	32.74	0.31%	28.50
436_9_3	**26.43**	30.16	0.21%	30.45	0.21%	29.78	0.20%	29.72	0.20%	29.22	0.18%	26.43
436_9_4	**25.18**	27.65	0.16%	27.38	0.16%	26.82	0.14%	28.20	0.16%	28.07	0.15%	25.18
872_9_2	43.38	36.95	6.96%	37.42	7.35%	37.73	6.38%	36.98	6.40%	**36.79**	5.18%	36.79
872_9_3	**30.49**	33.70	3.22%	33.21	3.35%	33.67	3.24%	32.78	3.00%	32.73	3.18%	30.49
872_9_4	**29.04**	31.11	2.27%	31.16	2.66%	31.46	2.60%	31.07	2.50%	30.96	2.41%	29.04
1744_9_2	70.93	47.06	10.57%	46.15	11.49%	**43.99**	12.61%	46.78	11.24%	46.99	9.80%	43.99
1744_9_3	58.76	44.35	13.71%	44.12	13.38%	**43.79**	14.95%	44.00	13.01%	43.85	12.69%	43.79
1744_9_4	54.10	**41.99**	12.85%	42.34	10.97%	42.21	10.52%	42.26	11.53%	42.93	11.56%	41.99

costs function are more noticeable with low to medium tolerance to the violation in $\mathcal{RC}$ and low in $\mathcal{UC}$. This means that even by allowing a medium tolerance for capacity constraints to be violated, both total operating costs and user costs are reduced on average.

4.2.3. Analysis of trends in violations of capacity constraints

To determine the extent to which the capacity constraints were violated in the soft configurations analysed, we study the trend of the average violations. Specifically, for each instance, we averaged the values of the τ variables over the Pareto Set and then aggregated these averages by the D parameter, as we observed similar trends when it varied. Table 8 reports this information as "average of avg(τ)" for each pair of λ s.

These data show that as expected, the average violations decrease as P increases, although for the *large* instances there is an increase when P goes from 2 to 3 which may be related to their specific topologies, making it difficult to satisfy the remaining constraints (as observed in Section 4.2.1). Another predictable result is the fact that, for each pair of λ values, the largest average violations occur on the *large* instances, which are characterised by numerous cells. However, as the number of available sites increases, the average violations decrease. This result is consistent with the fact that, as $|J|$ increases, the number of efficient solutions for the soft version of HWRC-Loc increases (cf. Section 4.2.1). Finally, the configurations with $\lambda_{\mathcal{RC}} = \lambda_{\mathcal{UC}} = -1$ and $\lambda_{\mathcal{RC}} = 0$ and $\lambda_{\mathcal{UC}} = -1$ lead to the highest average violations in percentage, regardless of the number of sites available. In particular comparing this trend, corresponding to a low to medium tolerance in $\mathcal{RC}$ and a low tolerance in $\mathcal{UC}$, with that of the other configurations, it can be concluded that tightening the tolerance thresholds allows the exploration of a closer neighbourhood of the initial feasible set thus leading to more drastic violations of the original constraints on the capacity of the systems.

To highlight the features of the different alternatives in the Pareto Sets of the soft version of the problem, we measure the maximum violation obtained for each instance and configuration of tolerance values. The relative data have been

Table 8. Average violations of capacity constraints (in percent) aggregated over D.

	Average of avg(τ)				
Cells_Sites_P	$\lambda_{\mathcal{RC}} = 0$ $\lambda_{\mathcal{UC}} = 0$	$\lambda_{\mathcal{RC}} = 0$ $\lambda_{\mathcal{UC}} = -1$	$\lambda_{\mathcal{RC}} = -1$ $\lambda_{\mathcal{UC}} = 0$	$\lambda_{\mathcal{RC}} = -1$ $\lambda_{\mathcal{UC}} = -1$	$\lambda_{\mathcal{RC}} = 0.5$ $\lambda_{\mathcal{UC}} = 0.5$
436_5_2	1.23%	1.23%	1.23%	1.23%	1.23%
436_5_3	0.69%	0.65%	0.65%	0.65%	0.65%
436_5_4	0.49%	0.51%	0.49%	0.49%	0.49%
872_5_2	16.72%	16.72%	16.72%	16.72%	16.72%
872_5_3	8.78%	8.78%	8.78%	8.78%	9.35%
872_5_4	6.68%	6.68%	6.68%	6.68%	6.68%
1744_5_2	–	–	–	–	–
1744_5_3	34.38%	34.38%	34.38%	34.38%	34.49%
1744_5_4	33.83%	33.93%	33.83%	33.83%	33.83%
436_7_2	0.55%	0.50%	0.50%	0.59%	0.55%
436_7_3	0.36%	0.40%	0.36%	0.38%	0.37%
436_7_4	0.27%	0.25%	0.26%	0.27%	0.25%
872_7_2	8.03%	8.03%	7.63%	8.21%	8.03%
872_7_3	5.20%	5.23%	5.20%	5.10%	5.10%
872_7_4	3.42%	3.29%	3.55%	3.47%	3.20%
1744_7_2	15.01%	15.01%	16.21%	16.21%	16.21%
1744_7_3	14.79%	17.94%	14.52%	15.74%	17.17%
1744_7_4	12.90%	13.39%	13.34%	14.03%	12.88%
436_9_2	0.33%	0.37%	0.36%	0.44%	0.31%
436_9_3	0.21%	0.21%	0.20%	0.20%	0.18%
436_9_4	0.16%	0.16%	0.14%	0.16%	0.15%
872_9_2	6.96%	7.35%	6.38%	6.40%	5.18%
872_9_3	3.22%	3.35%	3.24%	3.00%	3.18%
872_9_4	2.27%	2.66%	2.60%	2.50%	2.41%
1744_9_2	10.57%	11.49%	12.61%	11.24%	9.80%
1744_9_3	13.71%	13.38%	14.95%	13.01%	12.69%
1744_9_4	12.85%	10.97%	10.52%	11.53%	11.56%

Table 9. Maximum violation of capacity constraints (in percent) aggregated in terms of parameters D and P.

	Average maximum violation				
Cells_Sites	$\lambda_{\mathcal{RC}} = 0$ $\lambda_{\mathcal{UC}} = 0$	$\lambda_{\mathcal{RC}} = 0$ $\lambda_{\mathcal{UC}} = -1$	$\lambda_{\mathcal{RC}} = -1$ $\lambda_{\mathcal{UC}} = 0$	$\lambda_{\mathcal{RC}} = -1$ $\lambda_{\mathcal{UC}} = -1$	$\lambda_{\mathcal{RC}} = 0.5$ $\lambda_{\mathcal{UC}} = 0.5$
1744_5	132.18%	132.18%	132.18%	132.18%	131.44%
1744_7	123.00%	120.72%	122.97%	125.25%	125.25%
1744_9	134.23%	135.74%	143.87%	125.53%	129.85%

aggregated by D and P. For each configuration of λ s and value of $|J|$, the (average) maximum capacity violation is 10.47% on the *small* instances and 116.73% on the *medium* ones. Additionally, as observed for $avg(\tau)$, the largest (average) maximum violations relate to *large* instances, as reported in Table 9. In particular, although these violations are always above 100%, when $|J| = 7$ the corresponding values are lower, whilst the worst values are associated with $\lambda_{\mathcal{RC}} = \lambda_{\mathcal{UC}} = -1$ and $\lambda_{\mathcal{RC}} = -1$ and $\lambda_{\mathcal{UC}} = 0$.

We also analyse the component-wise percentage violation by counting the efficient solutions that have a violation of at most 10% (resp. 20%) on each component, i.e., such that $\| \tau\|_\infty = \max_{j\in J}|\tau_j| \leq 10\%$ (resp. $\| \tau\|_\infty \leq 20\%$). For any pair of λ s, as P increases, there are on average more solutions such that $\| \tau\|_\infty \leq 0.1$, although on the *large* instances with 9 candidates this trend is reversed when $\lambda_{\mathcal{RC}} = \lambda_{\mathcal{UC}} = 0$. Furthermore, for any fixed value of P and $|J|$, as $|I|$ increases, the percentage of solutions that satisfy the conditions on $\| \tau\|_\infty$ decreases, since the presence of more cells inevitably leads to potentially more active congested facilities. On the contrary, for any fixed value of P and $|I|$, this percentage increases as $|J|$ also increases. In fact, these results are consistent with the observations made for the average violation. The analysis also shows that no *large* solution with $|J| = 7, 9$ verifies $\| \tau\|_\infty \leq 0.2$, and this information is complementary to that extracted from Table 8, which highlights that all these instances have an average capacity violation below 20%.

In conclusion, this analysis confirmed that the average and maximum violations of the capacity constraints are sensitive to the instance size, the number of available candidates, and the tolerance thresholds.

Figure 5. Locations of the operating HWRCs in the city of Sheffield.

5. Case study: household waste recycling centres in Sheffield

This section describes the real case study based on the actual configuration of the HWRCs network in the city of Sheffield, South Yorkshire. Specifically, there are five operating HWRCs located in strategic positions (cf. Figure 5): Shirecliffe and Blackstock Road are the most central ones, while the remaining are located near the borders, thus being accessible to neighbouring areas (White, 2020; Zaharudin et al., 2021).

Analysis of the historical data reveals that the centres operate for 5–7 d a week, with 8-h shifts in summer and six-hour shifts in winter. This schedule ensures that at least two centres are operating each day.

To construct a real case study, we consider the geographical coordinates of the 1744 cells into which the city's households are aggregated. The values for capacity and operating costs were estimated by analysing confidential data provided by the WM team of the Sheffield City Council. Moreover, the threshold distance D is set to 80 by default (i.e., 8000 m), which corresponds to the maximum catchment radius for urban areas recommended by NACAS (WRAP, 2018a). By varying the set of candidate locations for the HWRCs and the value of P, we defined multiple configurations for conducting a *scenario-based analysis* and derive valuable managerial insights (Hu et al., 2017; Spinelli et al., 2025). Possible alternative candidates were selected from the Brownfield land register in consultation with the Sheffield City Council WM team.

The features of the scenarios are summarised in Table 10 and detailed below. In particular, they are obtained by simulating changes to the HWRCs

Table 10. Characteristics of the scenarios generated to conduct the managerial analysis.

ID	Name	$\|J\|$	P	Details on candidates in J
SR	Spending review	5	$\{2,3,4\}$	Actual centres of Sheffield
P-Re	Possible relocation	14	$\{2,3,4,5\}$	Actual centres of Sheffield and the nine centres of the `SH81` benchmark
LH	Larger HWRCs network	14	$\{6,7\}$	
LS	Larger Sites	20	$\{1,2,3\}$	With dimensions between 8 and 50 times those of Sheffield's HWRCs
Ro-C	Road Congestion	20	$\{2,3,4,5,6,7\}$	Belonging to a circular ring surrounding the city centre
RR	Restricted to Residents	15	$\{2,3,4,5\}$	Lying in a circle surrounding the city centre

network in terms of the number of facility sites (SR, LH), the size of the sites (LS, P-Re) and the network topology (Ro-C, RR).

Spending Review (SR): the candidates are the actual HWRCs of Sheffield but P varies in $\{2,3,4\}$ in order to simulate the closure of some operating centres.

Possible Relocation (P-Re): the set of 14 candidates comprises the five existing HWRCs in Sheffield and nine alternative candidates provided by the City Council to define the `SH81` benchmark (cf. Section 3.1); P varies within the set $\{2,3,4,5\}$. These scenarios simulate the possible relocation of one or more active HWRCs.

Larger HWRCs Network (LH): the set of candidates is the same as P-Re but $P = 6,7$ to simulate the opening of a greater number of centres.

Larger Sites (LS): there are 20 candidates each with a dimension between 8 and 50 times that of the actual HWRCs of Sheffield. The value of P varies within the set $\{1,2,3\}$ to simulate a network with fewer, larger centres.

Road Congestion (Ro-C): there are 20 candidates located in a circular ring around the city centre, while $P \in \{2,3,4,5,6,7\}$. These scenarios simulate a network design aimed at reducing road congestion in the city centre, caused by traffic near the HWRCs (Zaharudin et al., 2022).

Restricted to Residents (RR): there are 15 candidates in a circle around the city centre, and $P = 2,3,4,5$. These scenarios simulate a network design intended to prevent citizens from neighbouring areas from visiting the centres.

The experiments were conducted with the same settings described in Section 3.2, solving the soft version of the problem with $\lambda_{\mathcal{RC}} = \lambda_{\mathcal{UC}} = 0.5$. This choice is motivated by the need for a more realistic representation of these decision-making contexts, in order to provide the relevant stakeholders with concrete guidelines. To this end, we filtered the set of solutions to consider only those network configurations in which the capacity of each centre is exceeded by no more than 20%. In particular, the soft configuration with $\lambda_{\mathcal{RC}} = \lambda_{\mathcal{UC}} = 0.5$ potentially produces a significant number of efficient alternatives (cf. Section 4.2.1). Therefore, to support decision-makers in identifying the most suitable network configurations, we present the results of an analysis conducted on a reduced set of alternatives. They were selected using a method for *ranking and pruning* Pareto Sets, recently proposed by Dosantos et al. (2024). The method, known as *Order of Pareto Sets based on Borda Count* (OPSBC) is a versatile and impartial technique that exploits the properties of the Borda Count aggregation rule. The core idea is to construct solution rankings by treating each objective function as a voter, ordering the solutions from best to worst according to each objective function. These individual rankings are then aggregated by counting the number of times a solution is preferred over another across all rankings.

The analysis reported in Section 5.1 aims at demonstrating how the results of this research can provide stakeholders without technical expertise with the insights they need to make more informed decisions.

5.1. Managerial insights

The following observations relate to the analysis of the top three solutions obtained for each scenario, as ranked using the OPSBC method. The objective function values were chosen as key performance indicators (KPIs) to evaluate the performance of the corresponding network configurations.

5.1.1. HWRCs network configurations with fewer sites

Table 11 summarises the results for the SR scenarios with respect to the selected KPIs. A comparison of the objective function values shows that Sheffield's actual HWRCs network outperforms all possible alternative configurations in terms of user satisfaction with the service delivery system. Specifically, it achieves the highest coverage levels and the lowest user costs. Notably, the reduced number of active centres in the SR scenarios leads to an increase in the average distance between users and their nearest active site, by up to 42%. Conversely, alternative HWRCs network configurations with up to four centres naturally have reduced running costs. However, the aggregated results for SR3 show that limiting the number of active centres to three reduces running costs by 39%, while user costs and coverage worsen by 31% and 0.8%, respectively.

The tool offers managerial insights by showing that, under this parameter setting, on one hand, shutting existing centres could secure financial savings; on the other hand, it is also likely to negatively impact user satisfaction and the service network's compliance with legal requirements. A practical example of valuable solution for this class of

Table 11. Average values for the objective functions related to the SR scenarios. The number after the name of scenarios indicates the value of P. Objective function values for the Sheffield HWRCs network in the last column.

	SR2	SR3	SR4	Sheffield
avg ($\mathcal{UC}$)	519188.33	396928.67	433504.00	302572.00
avg ($\mathcal{RC}$)	57.67	99.67	98.33	164.00
avg ($\mathcal{CO}$)	9121.33	10186.33	10008.67	10266.00

scenarios is depicted in Figure 6, while the complete set of configurations for the different SR scenarios is given in Figure C1.

5.1.2. HWRCs network configurations with actual and alternative sites

The configurations selected for each P-Re scenario are depicted in Figure C2, while Table 12 shows the aggregated values for the KPIs.

The analysis shows that relocating some of the current centres would not improve the network's performance in terms of service quality. In fact, reducing the number of centres solely leads to lower (average) running costs (cf. P-Re2 to P-Re4), as already observed for the SR scenarios. Additionally, in all these configurations, the average values of the user costs are increased, by at most 92% (P-Re2).

However, the only configurations characterised by both alternative candidates and candidates from Sheffield's actual network are those obtained for scenario P-Re5. Indeed, solutions with five active centres always feature one alternative site whose activation improves $\mathcal{UC}$. In fact, the central gauges of the last row of solution plots in Figure C2 are the greenest. The managerial insights gained under this parameter setting suggest that relocating active centres can help mitigate the impact of potential HWRC closures on user satisfaction with service provision. In some cases, this approach can lead to milder trade-offs between service quality and financial savings compared to SR scenarios. This approach would be even more beneficial in terms of user costs and coverage when combined with the opening of two additional centres, as evidenced by the data in Table 13. However, managers should be aware that improving $\mathcal{UC}$ by up 10% may lead to an increase in HWRCs network running costs of between 78% and 360%, as can be seen from the colours of the gauges in Figure C3. Finally, Figure 7 shows a practical example of valuable solutions for the P-Re and LH scenarios.

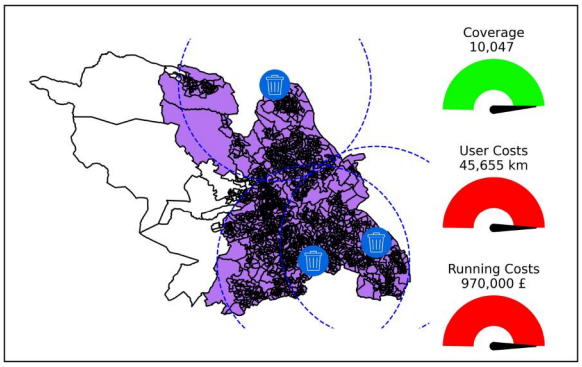

Figure 6. The solution to the SR scenario with $P = 4$ that ranked first in the OPSBC ranking. Covered cells are shown in purple and active HWRCs are depicted with a blue circle. The coverage area of each centre is represented by a dashed circle.

Table 12. Average values for the objective functions related to the P-Re scenarios. The number after the name of scenarios indicates the value of P. Objective function values for the Sheffield HWRCs network in the last column.

	P-Re2	P-Re3	P-Re4	P-Re5	Sheffield
avg($\mathcal{UC}$)	582617.33	437389.33	449206.33	349126.67	302572.00
avg($\mathcal{RC}$)	45.00	96.67	87.00	222.67	164.00
avg($\mathcal{CO}$)	8567.33	10096.00	10008.67	10189.00	10266.00

5.1.3. HWRCs network configurations with larger sites

Figure C4 presents the selected configurations for the LS scenarios. Notably, LS1 is characterised by a single efficient solution. As expected, network performance in terms of quality of service improves as P increases, although running costs are higher (cf. Section 3). Specifically, installing larger sites could increase running costs by an average of 750% compared to the current configuration of Sheffield's HWRCs network. Moreover, because such sites would need to be installed in large, potentially more dispersed areas, the average distance between users and their closest active centre would rise by 64% on average. The resulting network configurations achieve, on average, 91% coverage of total demand. Interestingly, among all the scenarios analysed, the LS configurations were the only ones in which no violations of capacity constraints were observed across all solutions. Under this parameter setting, the managerial insights suggest that reconfiguring

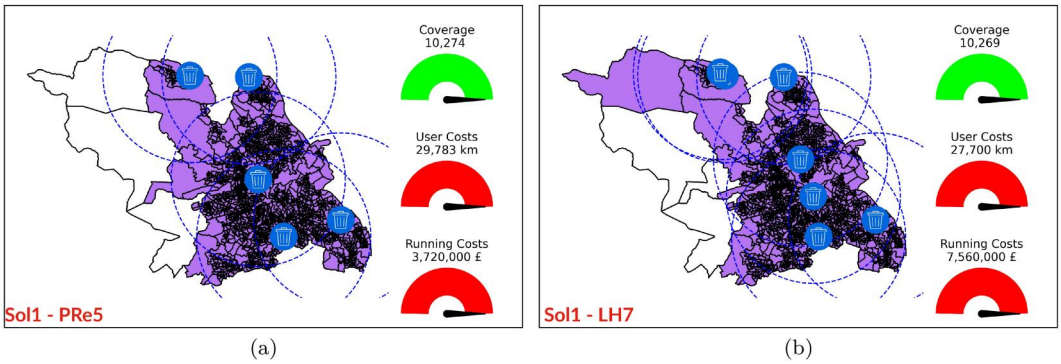

(a) (b)

Figure 7. Solutions that ranked first in the OPSBC ranking for scenarios P-Re5 (a) and LH7 (b).

Table 13. KPIs related to the LH scenarios. The number after the name of scenarios indicates the value of P. Table reports the number of current and alternative centres activated in each solution.

	LH6		LH7		Sheffield
	# Sheffield HWRCs	# Altern. HWRCs	# Sheffield HWRCs	# Altern. HWRCs	
	4	2	5	2	
$\mathcal{UC}$	314781		277003		302572
$\mathcal{RC}$	1276		756		164
$\mathcal{CO}$	10277		10269		10266
	3	0	3	0	
$\mathcal{UC}$	456548		456548		302572
$\mathcal{RC}$	97		97		164
$\mathcal{CO}$	10047		10047		10266
	3	0	5	2	
$\mathcal{UC}$	490518		272260		302572
$\mathcal{RC}$	92		294		164
$\mathcal{CO}$	9995		10266		10266

Table 14. Average values for the objective functions related to the Ro-C scenarios. The number after the name of scenarios indicates the value of P.

	Ro-C3	Ro-C4	Ro-C5	Ro-C6	Ro-C7
avg($\mathcal{UC}$)	393087.67	387178.50	351923.67	307724.33	281137.67
avg($\mathcal{RC}$)	1504.00	348.50	427.33	669.67	1094.00
avg($\mathcal{CO}$)	10197.67	10245.50	10254.33	10283.33	10275.33

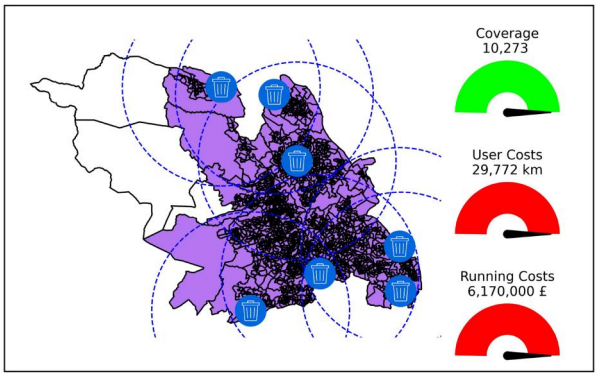

Figure 8. Solution that ranked first in the OPSBC ranking for scenarios Ro-C with $P = 7$.

the HWRCs network to include a limited number of larger sites may negatively impact performance across all KPIs.

5.1.4. HWRCs network configurations with alternative topologies

Table 14 reports the average of the KPIs for the Ro-C scenarios, which are characterised by candidates being located within a circular ring around the city centre. Notably, none of the configurations obtained for the Ro-C2 scenario adhered to the threshold imposed on the maximum capacity constraint violation for each site.

The analysis of the KPIs shows that the efficient HWRCs network configurations associated with these scenarios always cover at least the 99% of the total demand, equal to 10291. This is evident from the gauges associated with $\mathcal{CO}$ in Figure C5 which are always green.

Notably, the greater number of available sites has a significant impact on user costs and running costs as P increases. In fact, the capacity and running costs of centres depend on their size. When P is high enough, the model allows a greater number of centres to be activated, and among them there are centres with reduced capacities and running costs. For example, when P increases from three to seven, the corresponding average user costs ($\mathcal{UC}$) decrease by 28.5%, and $\mathcal{RC}$ by 27%.

Compared with the configurations obtained for scenarios with the same number of candidates (namely P-Re and LH), these are characterised by an average reduction in the distance between the user and the closest active centre of 13%. Although operating such networks may be more costly, the overall user experience could be enhanced, as evidenced by improved coverage and service quality under this parameter setting. Figure 8 presents a valuable network configuration obtained for the Ro-C7 scenario.

Conversely, topologies characterised by candidate sites located within a circular area surrounding the city centre inevitably lead to poorer performance of the HWRCs network across all KPIs. For example, the gauges associated with the values of $\mathcal{UC}$ in Figure C6 are always red, emphasising the significant deterioration in user experience in this type of HWRCs network topology. Switching from Ro-C to RR topologies increases the average distance between users and active centres, thereby raising user costs. However, the configurations generated by the model for the RR scenarios are associated with $\mathcal{CO}$ values averaging 93% of total demand. From a managerial perspective, these additional observations suggest that any network reconfiguration must carefully consider site locations. Specifically, to avoid negatively affecting network performance across certain KPIs, candidate sites should be selected so as to

avoid disadvantaging areas located further from the city centre.

5.1.5. Sensitivity analysis

To assess the robustness of the previous observations, and in line with the literature on case studies in WM field (Hu et al., 2017; Spinelli et al., 2025; Zhu et al., 2025), we conduct a sensitivity analysis of the results obtained. This process enables managers to make more informed decisions based on reliable insights.

To this end, we adapt the approach recently proposed by Forouli et al. (2022), which involves repeatedly solving the optimisation problem using AUGMECON-R, while applying percentage changes to the input parameters. Specifically, we perform 10 Monte Carlo simulations for each scenario, assuming that capacities, demands, running costs, and threshold distance follow a normal distribution with a standard deviation of $\pm 5\%$ (van de Ven et al., 2022). We analyse both the frequency of occurrence of solutions and the frequency of activation of the facility location variables, i.e., the x variables (cf. Section 2.2).

We define the *robustness* of a solution as the percentage of times it appears across the 10 Monte Carlo simulations. Table 15 shows the robustness of the solutions selected for each scenario according to the OPSBC method.

Analysis of these data highlights that the solutions from the SR and P-Re scenarios are the most robust, with average robustness percentages of 79% and 65%, respectively. Notably, among the three selected solutions, the most robust configurations for the P-Re4 and P-Re5 scenarios rank third and second, respectively. Conversely, the solutions obtained for the Ro-C and RR scenarios show the lowest robustness percentages, at 8% and 21% on average, respectively. This analysis suggests that, under this parameter setting, in the event of slight perturbations to the input data, the most reliable solutions arise from reconfigurations of the HWRCs network that retain the current sites. Furthermore, the simulations from the PR scenario indicate that these centres are more likely to remain active, even when relocation is considered.

We also examine the most robust solutions across the different configurations, considering those with a percentage occurrence of at least 50% to be robust. These data are summarised in Table 16. In particular, the most robust solutions for the P-Re, SR and LS scenarios are positioned in the second part of the ranking obtained using the OPSBC method. This implies that these solutions are not necessarily preferred to others with respect to all KPIs. For instance, SR configurations tend to have lower $\mathcal{RC}$ values on average, whereas P-Re configurations improve $\mathcal{UC}$ and $\mathcal{CO}$.

This analysis provides managers with complementary insights by identifying the configurations that are more stable in the face of input data

Table 15. Active centres, objective function values, and robustness for the solutions of the different scenarios. The order of listing reflects the OPSBC ranking of the solutions for each scenario.

Scenario	Active x	$\mathcal{UC}$	$\mathcal{RC}$	$\mathcal{CO}$	%robust.	Scenario	Active x	$\mathcal{UC}$	$\mathcal{RC}$	$\mathcal{CO}$	%robust.
SR2	x_1, x_3	506277	63	9969	100%	RR3	x_3, x_4	434717	215	9596	80%
	x_2, x_4	457325	72	9369	40%		x_9, x_{10}	444350	184	9453	0%
	x_4	593963	38	8026	80%		x_3, x_4, x_{10}	406749	304	9740	0%
SR3	x_0, x_3, x_4	369136	101	10266	90%	RR4	x_2, x_3, x_7, x_{10}	393546	531	9760	0%
	x_1, x_3, x_4	369136	101	10266	100%		$x_0, x_{10}, x_{12}, x_{14}$	379606	1058	9746	0%
	x_1, x_2, x_3	456548	97	10047	70%		x_0, x_9, x_{10}, x_{11}	389094	943	9733	0%
SR4	x_1, x_2, x_3	456548	97	10047	80%	RR5	x_3, x_7, x_8, x_{10}	390308	680	9760	0%
	x_0, x_1, x_3	490518	92	9995	90%		x_1, x_7, x_9, x_{12}	388545	668	9680	0%
	x_2, x_3, x_4	353446	106	9984	60%		x_0, x_2, x_3, x_{13}	403811	521	9611	0%
P-Re2	x_1, x_3	506277	63	9969	100%	LS2	x_7, x_9	493711	690	9549	0%
	x_4	593963	38	8026	50%		x_0, x_3	454565	2843	9131	80%
	x_3	647612	34	7707	90%		x_0, x_4	461624	3073	9173	40%
P-Re3	x_1, x_3, x_4	365102	101	10246	90%	LS3	x_1, x_7, x_9	425527	1809	9905	0%
	x_1, x_2, x_3	456548	97	10047	50%		x_{11}, x_{12}, x_{16}	395259	1799	9646	0%
	x_0, x_1, x_3	490518	92	9995	50%		x_9, x_{13}, x_{14}	476800	1230	9680	0%
P-Re4	x_1, x_2, x_3	456548	97	10047	50%	LS1	x_3	573215	366	8590	50%
	x_0, x_1, x_3	490518	92	9995	60%	Ro-C4	x_0, x_1, x_8, x_{17}	346183	478	10281	0%
	x_3, x_4	400553	72	9984	90%		x_1, x_2, x_3, x_6	428174	219	10210	0%
P-Re5	x_0, x_1, x_2, x_3, x_9	297827	372	10274	0%	Ro-C3	x_7, x_8, x_{13}	350468	1529	10057	0%
	x_1, x_2, x_3, x_4, x_5	293005	199	10246	90%		x_5, x_{10}, x_{17}	389313	1518	10268	0%
	x_1, x_2, x_3	456548	97	10047	60%		x_4, x_6, x_{10}	439482	1465	10268	0%
LH6	$x_3, x_4, x_5, x_9, x_{10}, x_{11}$	314781	1276	10277	0%	Ro-C5	x_1, x_3, x_6, x_8, x_9	342254	398	10217	0%
	x_1, x_2, x_3	456548	97	10047	40%		x_0, x_3, x_4, x_5, x_8	330288	620	10272	0%
	x_0, x_1, x_3	490518	92	9995	0%		x_0, x_1, x_2, x_3, x_6	383229	264	10274	70%
LH7	$x_0, x_1, x_2, x_3, x_4, x_5, x_{11}$	277003	756	10269	0%	Ro-C6	$x_0, x_2, x_5, x_8, x_{14}, x_{16}$	301858	457	10288	0%
	x_1, x_2, x_3	456548	97	10047	50%		$x_0, x_1, x_2, x_3, x_6, x_8$	325458	407	10281	40%
	$x_0, x_1, x_2, x_3, x_4, x_5, x_6$	272260	294	10266	100%		$x_1, x_6, x_8, x_9, x_{13}$	295857	1145	10281	0%
RR2	x_3, x_4	434717	215	9596	60%	Ro-C7	$x_0, x_1, x_2, x_5, x_9, x_{11}, x_{17}$	297723	617	10273	0%
	x_1, x_3	462437	195	9422	90%		$x_2, x_6, x_8, x_9, x_{16}, x_{17}$	273033	674	10281	0%
							$x_3, x_4, x_6, x_7, x_8, x_9, x_{13}$	272657	1991	10272	0%

Table 16. Active centres and objective function values for solutions with a robustness score of at least 50%. The final columns show the OPSBC ranking of solutions that also solved the original problem and the total number of solutions.

Scenario	Active x	$\mathcal{UC}$	$\mathcal{RC}$	$\mathcal{CO}$	%robust.	Ranking	#Sol.
SR3	x_4	593963	38	8026	100%	7	9
	x_3	647612	34	7707	100%	8	
	x_1, x_3	506277	63	9969	100%	5	
SR4	x_0, x_1, x_3, x_4	349679	130	10266	100%	9	12
	x_3	647612	34	7707	100%	7	
P-Re3	x_1, x_3	506277	63	9969	100%	5	9
	x_3, x_4	400553	72	9984	100%	4	
P-Re4	x_1, x_3	506277	63	9969	100%	4	11
	x_1, x_3, x_4	365102	101	10246	100%	10	
	x_0, x_1, x_3, x_4	349679	130	10266	100%	8	
	x_0, x_2, x_3, x_4	322029	135	10266	100%	9	
	x_0, x_3, x_4	369136	101	10266	100%	11	
P-Re5	x_0, x_1, x_3, x_4	349679	130	10266	100%	10	13
	x_0, x_2, x_3, x_4	322029	135	10266	100%	11	
	x_0, x_1, x_2, x_3, x_4	302572	164	10266	100%	12	
LH6	x_1, x_3	506277	63	9969	100%	7	18
	x_0, x_2, x_3, x_4	322029	135	10266	100%	16	
	x_0, x_1, x_2, x_3, x_4	302572	164	10266	100%	4	
	$x_0, x_1, x_2, x_3, x_4, x_5$	297039	199	10266	100%	5	
	x_1, x_3, x_4	365102	101	10246	100%	9	
	x_0, x_1, x_3, x_4	349679	130	10266	100%	12	
	x_1, x_2, x_3, x_4	317995	135	10246	100%	15	
LH7	x_0, x_2, x_3, x_4	322029	135	10266	100%	22	23
	x_0, x_1, x_2, x_3, x_4	302572	164	10266	100%	9	
	$x_0, x_1, x_2, x_3, x_4, x_5$	297039	199	10266	100%	4	
	x_3	647612	34	7707	100%	None	
	x_1, x_3	506277	63	9969	100%	7	
	x_1, x_2, x_3, x_4, x_5	293005	199	10246	100%	16	
LS2	x_3	573215	366	8590	90%	None	5
LS3	x_3	573215	366	8590	90%	7	8
	x_5	598585	541	8636	50%	8	
Ro-C7	$x_0, x_1, x_2, x_3, x_4, x_5, x_8$	304215	677	10281	50%	None	14
RR3	x_1, x_3, x_4	426994	311	9596	90%	None	4
RR4	x_1, x_3	462437	195	9422	90%	5	12
	x_1, x_3, x_4	426994	311	9596	70%	None	
RR5	x_3, x_4	434717	215	9596	80%	9	14
	x_1, x_3	462437	195	9422	70%	4	

Table 17. Frequency of activation of the location variables across the 10 Monte Carlo simulations. The final columns show the OPSBC ranking of solutions that also solved the original problem and the total number of solutions.

SR		P-Re		LH		LS		Ro-C		RR	
Var.	#Occur.	Var.	#Occur.	Var.	#Occur.	Var.	#Occur.	Var.	#Occur.	Var.	#Occur.
x_0	68	x_0	137	x_0	210	x_0	50	x_0	362	x_0	76
x_1	103	x_1	169	x_1	219	x_1	20	x_1	272	x_1	107
x_2	82	x_2	143	x_2	240	x_2	9	x_2	270	x_2	57
x_3	192	x_3	348	x_3	338	x_3	77	x_3	374	x_3	197
x_4	141	x_4	258	x_4	287	x_4	28	x_4	142	x_4	108
		x_5	23	x_5	74	x_5	45	x_5	204	x_5	27
		x_6	6	x_6	30	x_6	21	x_6	282	x_6	7
		x_7	7	x_7	18	x_7	46	x_7	78	x_7	43
		x_9	19	x_8	2	x_8	11	x_8	330	x_8	13
		x_{11}	4	x_9	53	x_9	19	x_9	100	x_9	45
		x_{13}	3	x_{10}	4	x_{10}	16	x_{10}	36	x_{10}	92
				x_{11}	6	x_{11}	2	x_{11}	62	x_{11}	28
				x_{12}	4	x_{12}	9	x_{12}	25	x_{12}	40
				x_{13}	8	x_{13}	4	x_{13}	68	x_{13}	12
						x_{14}	3	x_{14}	59	x_{14}	13
						x_{15}	3	x_{15}	51		
						x_{16}	1	x_{16}	64		
						x_{17}	5	x_{17}	60		
						x_{19}	2	x_{18}	7		
								x_{19}	34		

perturbations. This enables them to make more informed decisions by combining suggestions from Pareto Set rankings with stability analysis indications.

Finally, we analyse the frequency with which the x decision variables are activated across the 10 Monte Carlo simulations. The aim is to identify the centres most likely to be activated in each type of scenario. Table 17 reports this information.

For example, under the parameters setting considered, the data suggest that when reconfiguring Sheffield's current HWRC network – while

retaining its existing centres among the candidate sites – centres 3 and 4 are the most likely to remain active (see SR, P-Re, and LH scenarios). Similar insights can be drawn for the remaining scenarios.

6. Conclusions

The HWRCs are facilities that provide multiple services to residents: collection, re-use, and recycling of bulky waste. Therefore, the HWRCs network should be carefully designed in order to ensure efficient running and proper utilisation of these facilities by residents, thus encouraging their participation in recycling plans. Although the UK government is aware of this, the ongoing financial cuts affecting the public sector are severely challenging the efficient and cost-effective operation of the HWRCs network in several cities. At this purpose, Sheffield City Council in South Yorkshire aims to explore new configurations for its current system of waste recycling centres, potentially identifying efficient locations for additional sites, with the dual aim of reducing operating costs and improving user satisfaction.

In doing so, we formalise the decision-making process underlying this specific real-world case study. To this end, in the present paper we define and model a novel Multi-Objective Facility Location Problem in WM, dealing with determining the location of a predefined number of HWRCs capacitated facilities and allocating demand accordingly, in order to meet the legislative requirements concerning the user-site distance. In particular, this problem owes its Multi-Objective nature to the fact that the objective functions incorporate the possibly conflicting interests of the different stakeholders involved in the process. Furthermore, with the aim of representing the actual dynamics leading the workflow of design and operation, we devise a soft-constrained approach to the arising problem, allowing the violation of the capacity constraints. Finally, in order to provide the authorities involved in this collaboration with a feasibility study of the proposed approaches, we derive a real-world case study based on the actual configuration of the Sheffield HWRCs network and conduct a scenario-based analysis simulating different network reconfigurations.

The relevant Pareto Sets of both the original problem and its soft-constrained version are explored by tailoring the robust version of the AUGMEnted ε-CONstraint method (AUGMECON-R) (Nikas et al., 2022). From the thorough analysis of the numerical results we derive valuable information that is of significant operational and managerial value. First, we notice that tighter coverage thresholds can reduce the compliance of the service network with legislative requirements related to user-site distance, thus challenging the resolution of the problem. We also find that the capacity constraints become harder to satisfy as the number of users increases. In this context, the introduction of soft capacity constraints turns out to be instrumental in reducing solution times and providing larger Pareto Sets. In addition, both coverage and user satisfaction are positively affected by the relaxation of capacity constraints, even when they are not excessively violated; however, surprisingly, this approach also leads to lower average running costs, as network configurations that were originally infeasible become feasible.

We undertake scenario and sensitivity analyses for a real-world case study, as an example to showcase the benefits of adopting the proposed tool to gather practical and actionable guidance and support policy making. Subject to the specific setting of parameters adopted in these particular experiments, various HWRCs reconfiguration scenarios are considered. The results enable the efficient exploration of the trade-offs between financial savings and the quality of the service provision associated with a range of different reconfiguration options. Furthermore, the tool facilitates careful site selection to ensure that more remote areas are not disproportionately affected during the reconfiguration of the HWRC network.

In conclusion, the research presented in this paper proved capable of meeting the needs arising from the real-case study, through the solution of benchmark instances obtained from real data provided by Sheffield City Council. Indeed, being the number of Pareto optimal solutions contained, the Multi-Objective modelling approach proves effective in supporting concrete decision-making. In fact, the policy makers can choose the HWRCs network configuration from a limited set of efficient alternatives. This choice can be even facilitated by the use of a *ranking* method: to this end, we have also adapted an approach recently proposed in Dosantos et al. (2024), which allows to rank efficient solutions using the Borda count aggregation rule.

In terms of future research directions, it could be interesting to define new tailored classes of budget constraints based on the NACAS guidelines (WRAP, 2018a) and to integrate a diversification of facility types, possibly including supersites that can also collect waste from neighbouring cities. From a computational point of view, it could be useful to investigate the performance of AUGMECON-R in solving significantly larger instances and to explore the need for heuristic approaches. Finally, since an extended set of efficient alternatives might be

difficult to interpret, the developed decision support system would benefit from an ad hoc clustering of the Pareto Sets (Kahagalage et al., 2023; Seyedashraf et al., 2023), aimed at identifying similarities between solutions and selecting a representative set of alternatives.

Acknowledgements

The authors are grateful to Mr Neil Townrow, Mr Andrew France, Ms Bobbie Gardner, and Mr Alistair Black from the WM Team of the Sheffield City Council for supporting this work by describing and discussing the underlying real-world problem with the authors, and by providing valuable information to generate the dataset utilised in the Case Study.

The authors would like to thank the anonymous referees for their valuable comments, which contributed to improving the quality of this article.

This research was partially supported by the project "Promoting Sustainable Freight Transport in Urban Contexts: Policy and Decision-Making Approaches (ProSFeT)", funded by the H2020-MSCA-RISE-2016 programme (Grant Number: 734909). This support is gratefully acknowledged.

Disclosure statement

There are no interests to declare.

Funding

This research was partially supported by the project "Promoting Sustainable Freight Transport in Urban Contexts: Policy and Decision-Making Approaches (ProSFeT)", funded by the H2020-MSCA-RISE-2016 programme (Grant Number: 734909).

References

Adeleke, O. J., & Olukanni, D. O. (2020). Facility location problems: Models, techniques, and applications in waste management. *Recycling*, *5*(2), 10. https://doi.org/10.3390/recycling5020010

Ahluwalia, P. K., & Nema, A. K. (2011). Capacity planning for electronic waste management facilities under uncertainty: Multi-objective multi-time-step model development. *Waste Management and Research*, *29*(7), 694–709.

Alumur, S., & Kara, B. Y. (2007). A new model for the hazardous waste location-routing problem. *Computers & Operations Research*, *34*(5), 1406–1423. https://doi.org/10.1016/j.cor.2005.06.012

Archetti, C., Guerriero, F., & Macrina, G. (2021). The online vehicle routing problem with occasional drivers. *Computers & Operations Research*, *127*, 105144. https://doi.org/10.1016/j.cor.2020.105144

Asghari, M., Fathollahi-Fard, A. M., Mirzapour Al-E-Hashem, S., & Dulebenets, M. A. (2022). Transformation and linearization techniques in optimization: A state-of-the-art survey. *Mathematics*, *10*(2), 283. https://doi.org/10.3390/math10020283

Barisone, A., Black, A., Crimi, A., Genovese, A., Gorini, M., Jones , & Stella, L. (2019). *A report about practical implementation of decision support systems for freight transport planning in real-world contexts*. ProSFeT. Project, Report 2.2.

BBC. (2016). *Sheffield bin workers walk out in 24-hour strike action over pay*. BBC.

Church, R. L., & Cohon, J. L. (1976). *Multi-objective location analysis of regional energy facility siting problems* (No. BNL-50567). Brookhaven National Lab.

Darmian, S. M., Moazzeni, S., & Hvattum, L. M. (2020). Multi-objective sustainable location-districting for the collection of municipal solid waste: Two case studies. *Computers & Industrial Engineering*, *150*, 106965. https://doi.org/10.1016/j.cie.2020.106965

Daskin, M. S. (2011). *Network and discrete location: Models, algorithms, and applications*. John Wiley & Sons.

De Feo, G., & De Gisi, S. (2010). Public opinion and awareness towards MSW and separate collection programmes: A sociological procedure for selecting areas and citizens with a low level of knowledge. *Waste Management (New York, NY)*, *30*(6), 958–976. https://doi.org/10.1016/j.wasman.2010.02.019

Department for Environment Food and Rural Affairs. (2019). *Consistency in recycling collections in England: Executive summary and government response*. GOV.UK. [Link].

Department for Environment Food and Rural Affairs. (2020). *UK statistics on waste*. GOV.UK. [Link].

Dosantos, P. S., Bouchet, A., Mariñas-Collado, I., & Montes, S. (2024). OPSBC: A method to sort Pareto-optimal sets of solutions in multi-objective problems. *Expert Systems with Applications*, *250*, 123803. https://doi.org/10.1016/j.eswa.2024.123803

Ehrgott, M., & Tenfelde-Podehl, D. (2003). Computation of ideal and nadir values and implications for their use in MCDM methods. *European Journal of Operational Research*, *151*(1), 119–139. https://doi.org/10.1016/S0377-2217(02)00595-7

Engkvist, I. L., Eklund, J., Krook, J., Björkman, M., & Sundin, E. (2016). Perspectives on recycling centres and future developments. *Applied Ergonomics*, *57*, 17–27. https://doi.org/10.1016/j.apergo.2016.01.001

Erkut, E., Karagiannidis, A., Perkoulidis, G., & Tjandra, S. A. (2008). A multicriteria facility location model for municipal solid waste management in North Greece. *European Journal of Operational Research*, *187*(3), 1402–1421. https://doi.org/10.1016/j.ejor.2006.09.021

Espejo, I., Marín, A., & Rodríguez-Chía, A. M. (2012). Closest assignment constraints in discrete location problems. *European Journal of Operational Research*, *219*(1), 49–58. https://doi.org/10.1016/j.ejor.2011.12.002

Estrada-Moreno, A., Ferrer, A., Juan, A. A., Bagirov, A., & Panadero, J. (2020). A biased-randomised algorithm for the capacitated facility location problem with soft constraints. *Journal of the Operational Research Society*, *71*(11), 1799–1815. https://doi.org/10.1080/01605682.2019.1639478

Forouli, A., Pagonis, A., Nikas, A., Koasidis, K., Xexakis, G., Koutsellis, T., Petkidis, C., & Doukas, H. (2022). AUGMECON-Py: A python framework for multi-objective linear optimisation under uncertainty. *SoftwareX*, *20*, 101220. https://doi.org/10.1016/j.softx.2022.101220

Fugaro, S., & Sgalambro, A. (2023). Advanced network connectivity features and zonal requirements in

Covering Location problems. *Computers & Operations Research*, *159*, 106307. https://doi.org/10.1016/j.cor.2023.106307

Fugaro, S., & Sgalambro, A. (2025). *Multi-objective facility location problems: Systematic literature review and research agenda*. Elsevier. Available at SSRN 5178615.

Garey, M. R., & Johnson, D. S. (1979). *Computers and intractability: A guide to the theory of NP-completeness*. W. H. Freeman and Company.

Ghiani, G., Laganà, D., Manni, E., & Triki, C. (2012). Capacitated location of collection sites in an urban waste management system. *Waste Management (New York, NY)*, *32*(7), 1291–1296. https://doi.org/10.1016/j.wasman.2012.02.009

Habibi, F., Asadi, E., Sadjadi, S. J., & Barzinpour, F. (2017). A multi-objective robust optimization model for site-selection and capacity allocation of municipal solid waste facilities: A case study in Tehran. *Journal of Cleaner Production*, *166*, 816–834. https://doi.org/10.1016/j.jclepro.2017.08.063

Han, L., Xu, D., Xu, Y., & Zhang, D. (2020). Approximating the τ-relaxed soft capacitated facility location problem. *Journal of Combinatorial Optimization*, *40*(3), 848–860. https://doi.org/10.1007/s10878-020-00631-y

His Majesty Government. (2018). *A green future: Our 25 year plan to improve the environment*. His Majesty Government.

Hu, C., Liu, X., & Lu, J. (2017). A bi-objective two-stage robust location model for waste-to-energy facilities under uncertainty. *Decision Support Systems*, *99*, 37–50. https://doi.org/10.1016/j.dss.2017.05.009

Isermann, H., & Steuer, R. E. (1988). Computational experience concerning payoff tables and minimum criterion values over the efficient set. *European Journal of Operational Research*, *33*(1), 91–97. https://doi.org/10.1016/0377-2217(88)90257-3

Kahagalage, S., Turan, H. H., Jalalvand, F., & El Sawah, S. (2023). A novel graph-theoretical clustering approach to find a reduced set with extreme solutions of Pareto optimal solutions for multi-objective optimization problems. *Journal of Global Optimization*, *86*(2), 467–494. https://doi.org/10.1007/s10898-023-01275-y

Kailomsom, P., & Khompatraporn, C. (2023). A multi-objective optimization model for multi-facility decisions of infectious waste transshipment and disposal. *Sustainability*, *15*(6), 4808. https://doi.org/10.3390/su15064808

Local Government Association. (2018). *Resources and waste strategy summary*. LOCAL.GOV.UK.

Ma, Y., Zhang, W., Feng, C., Lev, B., & Li, Z. (2021). A bi-level multi-objective location-routing model for municipal waste management with obnoxious effects. *Waste Management (New York, NY)*, *135*, 109–121. https://doi.org/10.1016/j.wasman.2021.08.034

Mavrotas, G. (2009). Effective implementation of the ε-constraint method in multi-objective mathematical programming problems. *Applied Mathematics and Computation*, *213*(2), 455–465. https://doi.org/10.1016/j.amc.2009.03.037

Mavrotas, G., & Florios, K. (2013). An improved version of the augmented ε-constraint method (AUGMECON2) for finding the exact pareto set in multi-objective integer programming problems. *Applied Mathematics and Computation*, *219*(18), 9652–9669. https://doi.org/10.1016/j.amc.2013.03.002

Nikas, A., Fountoulakis, A., Forouli, A., & Doukas, H. (2022). A robust augmented ε-constraint method (AUGMECON-R) for finding exact solutions of multi-objective linear programming problems. *Operational Research*, *22*, 1291–1332. https://doi.org/10.1007/s12351-020-00574-6

Office for National Statistics. (2011). *Census 2011*. ONS. [Link].

Oluwadipe, S., Garelick, H., McCarthy, S., & Purchase, D. (2022). A critical review of household recycling barriers in the United Kingdom. *Waste Management & Research: The Journal of the International Solid Wastes and Public Cleansing Association, ISWA*, *40*(7), 905–918. https://doi.org/10.1177/0734242X211060619

Pisacane, O., Potena, D., Antomarioni, S., Bevilacqua, M., Ciarapica, F. E., & Diamantini, C. (2021). Data-driven predictive maintenance policy based on multi-objective optimization approaches for the component repairing problem. *Engineering Optimization*, *53*(10), 1752–1771. https://doi.org/10.1080/0305215X.2020.1823381

Sáez-Aguado, J., & Trandafir, P. C. (2018). Variants of the ε-constraint method for biobjective integer programming problems: Application to p-median-cover problems. *Mathematical Methods of Operations Research*, *87*(2), 251–283. https://doi.org/10.1007/s00186-017-0618-9

Samanlioglu, F. (2013). A multi-objective mathematical model for the industrial hazardous waste location-routing problem. *European Journal of Operational Research*, *226*(2), 332–340. https://doi.org/10.1016/j.ejor.2012.11.019

Seyedashraf, O., Bottacin-Busolin, A., & Harou, J. J. (2023). Assisting decision-makers select multi-dimensionally efficient infrastructure designs–Application to urban drainage systems. *Journal of Environmental Management*, *336*, 117689. https://doi.org/10.1016/j.jenvman.2023.117689

Shi, J., Wang, R., Chen, W., Xing, L., & Jin, M. (2020). Bi-objective design of household E-waste collection with public advertising and competition from informal sectors. *Waste Management (New York, NY)*, *102*, 65–75. https://doi.org/10.1016/j.wasman.2019.10.018

Shokouhyar, S., & Aalirezaei, A. (2017). Designing a sustainable recovery network for waste from electrical and electronic equipment using a genetic algorithm. *International Journal of Environment and Sustainable Development*, *16*(1), 60–79. https://doi.org/10.1504/IJESD.2017.080851

Smith, L. (2023). *Fly-tipping: The illegal dumping of waste*. House of Commons Library.

Smith, L., & Bolton, P. (2018). *Household recycling in the UK*. House of Commons Library.

Spinelli, A., Maggioni, F., Ramos, T., Barbosa-Póvoa, A. P., & Vigo, D. (2025). A rolling horizon heuristic approach for a multi-stage stochastic waste collection problem. *European Journal of Operational Research*, *323*(1), 276–296. https://doi.org/10.1016/j.ejor.2024.11.041

Tari, I., & Alumur, S. A. (2014). Collection center location with equity considerations in reverse logistics networks. *Information Systems and Operational Research*, *52*, 4. https://doi.org/10.3138/infor.52.4.157

Tautenhain, C. P., Barbosa-Povoa, A. P., & Nascimento, M. C. (2019). A multi-objective matheuristic for designing and planning sustainable supply chains. *Computers & Industrial Engineering*, *135*, 1203–1223. https://doi.org/10.1016/j.cie.2018.12.062

Tralhão, L., Coutinho-Rodrigues, J., & Alçada-Almeida, L. (2010). A multiobjective modeling approach to locate multi-compartment containers for urban-sorted waste.

Waste Management (New York, NY), *30*(12), 2418–2429. https://doi.org/10.1016/j.wasman.2010.06.017

van de Ven, D.-J., Nikas, A., Koasidis, K., Forouli, A., Cassetti, G., Chiodi, A., Gargiulo, M., Giarola, S., Köberle, A. C., Koutsellis, T., Mittal, S., Perdana, S., Vielle, M., Xexakis, G., Doukas, H., & Gambhir, A. (2022). COVID-19 recovery packages can benefit climate targets and clean energy jobs, but scale of impacts and optimal investment portfolios differ among major economies. *One Earth (Cambridge, MA)*, *5*(9), 1042–1054. https://doi.org/10.1016/j.oneear.2022.08.008

Wang, J., Cevik, M., Amin, S. H., & Parsaee, A. A. (2021). Mixed-integer linear programming models for the paint waste management problem. *Transportation Research Part E: Logistics and Transportation Review*, *151*, 102343. https://doi.org/10.1016/j.tre.2021.102343

White, R. (2020). *Sheffield implements fines for HWRC queues*. Letsrecycle.

Wichapa, N., & Khokhajaikiat, P. (2017). Using the hybrid fuzzy goal programming model and hybrid genetic algorithm to solve a multi-objective location routing problem for infectious waste disposal. *Journal of Industrial Engineering and Management*, *10*(5), 853–886. https://doi.org/10.3926/jiem.2353

Wichapa, N., & Khokhajaikiat, P. (2018). Solving a multi-objective location routing problem for infectious waste disposal using hybrid goal programming and hybrid genetic algorithm. *International Journal of Industrial Engineering Computations*, *9*(1), 75–98. https://doi.org/10.5267/j.ijiec.2017.4.003

WRAP. (2018a). *Household waste recycling centre (HWRC) guide*. WRAP.

WRAP. (2018b). *Summary: Wrap household waste recycling centres (HWRC) guide*. WRAP.

Zaharudin, Z. A., Brint, A., & Genovese, A. (2022). A multi-period model for reorganising urban household waste recycling networks. *Socio-Economic Planning Sciences*, *84*, 101396. https://doi.org/10.1016/j.seps.2022.101396

Zaharudin, Z. A., Brint, A., Genovese, A., & Piccolo, C. (2021). A spatial interaction model for the representation of user access to household waste recycling centres. *Resources, Conservation and Recycling*, *168*, 105438. https://doi.org/10.1016/j.resconrec.2021.105438

Zhao, J., Huang, L., Lee, D. H., & Peng, Q. (2016). Improved approaches to the network design problem in regional hazardous waste management systems. *Transportation Research Part E: Logistics and Transportation Review*, *88*, 52–75. https://doi.org/10.1016/j.tre.2016.02.002

Zhao, J., Wu, B., & Ke, G. Y. (2021). A bi-objective robust optimization approach for the management of infectious wastes with demand uncertainty during a pandemic. *Journal of Cleaner Production*, *314*, 127922. https://doi.org/10.1016/j.jclepro.2021.127922

Zhu, A., Wang, X., Fan, Y., & Liang, L. (2025). Value-based disposal mechanism for relief supply returns in post-disaster humanitarian logistics. *Journal of the Operational Research Society*, 1–14. https://doi.org/10.1080/01605682.2025.2460659

Appendices

Appendix A. On the inherent multi-objective nature of the HWRC-Loc

As reported in Section 2.2, it is reasonable to expect that the trend of the running costs function $\mathcal{RC}$ will be opposite to that of the other objectives which refer to the quality of service provision. However, the criterion used to define the cells, i.e., the aggregation of citizens, and the definition of the demand function h may result in demand values that are possibly not uniformly distributed. As a consequence, minimising $\mathcal{UC}$ can also conflict with maximising $\mathcal{CO}$, as shown in the following example.

Consider an instance of HWRC-Loc featuring two facility sites, a and b, and two demand nodes, i and j; we assume that the running costs for the facility sites coincide and that at most one facility has to be located, i.e., $P = 1$. Moreover, $N_i = \{a\}$, $N_j = \emptyset$, and $h_i \lll h_j$ (cf. Figure A1).

If the facility were to be located in a, $\mathcal{CO}(a) = h_i$ and $\mathcal{UC}(a) = d_{ia}h_i + d_{ja}h_j$; instead, locating the facility in b would yield to $\mathcal{CO}(b) = 0$ and $\mathcal{UC}(b) = d_{ib}h_i + d_{jb}h_j$. The assumption on the demand values, along with the distance between j and a being greater than the distance between j and b implies that $\mathcal{UC}(a) > \mathcal{UC}(b)$. Therefore, the former choice of the facility site optimises $\mathcal{CO}$, the latter $\mathcal{UC}$.

Appendix B

AUGMECON-R framework for the household waste recycling centres location problem

The core of the AUGMECON-R technique consists in the iterative solution of a SOP, obtained from the Multi-Objective problem to be solved initially. In order to obtain the mathematical formulation of an SOP associated with the HWRC-Loc, let us assume that $\mathcal{UC}$ is optimised

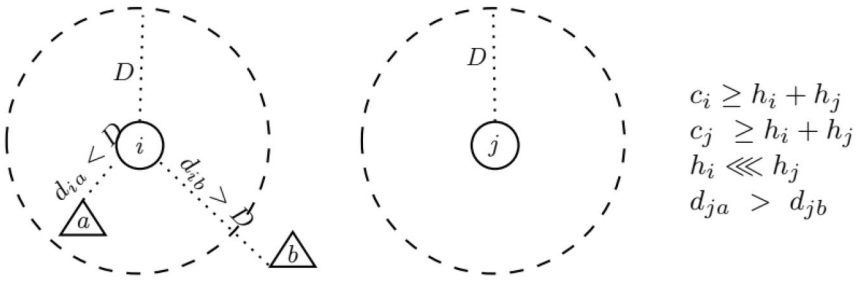

Figure A1. Demand nodes drawn as circles, facility sites as triangles. Dashed rings contain demand nodes and the sites that can cover them. Hypotheses and conditions for parameters shown on the right-hand side.

in the objective function of this problem, and that the optimisation of $\mathcal{CO}$ is prioritised over that of $\mathcal{RC}$. Furthermore, to simplify the interpretation of the output solutions, we replace the function $\mathcal{CO}$ by $-\mathcal{CO}$, so that all functions have to be minimised. The following variables and parameters are essential in formulating the SOP:

1. non-negative slack variables $S_{\mathcal{CO}}$ and $S_{\mathcal{RC}}$ associated with $-\mathcal{CO}$ and $\mathcal{RC}$, respectively;
2. positive parameters $r_{\mathcal{CO}}$ and $r_{\mathcal{RC}}$ denoting the *ranges* of $-\mathcal{CO}$ and $\mathcal{RC}$, i.e., absolute differences between the best and worst possible values (cf. Remark 2);
3. parameters $\varepsilon_{\mathcal{CO}}$ and $\varepsilon_{\mathcal{RC}}$ representing the threshold values for $-\mathcal{CO}$ and $\mathcal{RC}$.

The resulting Single-Objective Mixed Integer Linear Program is given in (B1).

$$(\text{SOP}) \min \left[\mathcal{UC} - \delta * \left(\frac{S_{\mathcal{CO}}}{r_{\mathcal{CO}}} + 10^{-1} \frac{S_{\mathcal{RC}}}{r_{\mathcal{RC}}} \right) \right] \tag{B1a}$$

$$\begin{gathered} \text{subject to} \\ \text{Constraints } (1\text{d}) - (1\text{f}),\ (1\text{h}) - (1\text{i}),\ (2) \\ -\mathcal{CO} + S_{\mathcal{CO}} = \varepsilon_{\mathcal{CO}} \end{gathered} \tag{B1b}$$

$$\mathcal{RC} + S_{\mathcal{RC}} = \varepsilon_{\mathcal{RC}} \tag{B1c}$$

$$S_{\mathcal{CO}}, S_{\mathcal{RC}} \geq 0 \tag{B1d}$$

Constraints (B1b)-(B1c) are the parametric ε-constraints, where the values of the parameters vary over the iterations, by defining a two-dimensional grid of equally spaced points in the solution space, each corresponding to a pair of $(\varepsilon_{\mathcal{CO}}, \varepsilon_{\mathcal{RC}})$ values (Mavrotas, 2009). The *discretisation step* for this grid is obtained by dividing the range of each function in $(q_l - 1)$ intervals, $l = \mathcal{CO}, \mathcal{RC}$, and the ε values are obtained as in (B2), where $i_l = 0, \ldots q_l$.

$$\varepsilon_{\mathcal{CO}} = \max[-\mathcal{CO}] - i_{\mathcal{CO}} * \frac{r_{\mathcal{CO}}}{q_{\mathcal{CO}}},$$

$$\varepsilon_{\mathcal{RC}} = \max \mathcal{RC} - i_{\mathcal{RC}} * \frac{r_{\mathcal{RC}}}{q_{\mathcal{RC}}} \tag{B2}$$

In correspondence with the solution of a feasible SOP, the so-called *bypass coefficients* are computed as reported in (B3): they represent the number of iterations of the corresponding loop on the ε parameters to skip in order to avoid the resolution of redundant SOPs (Nikas et al., 2022).

$$b_l = \left\lfloor S_l * \frac{r_l}{q_l} \right\rfloor, \quad l = \mathcal{CO}, \mathcal{RC} \tag{B3}$$

Algorithm 1 reports the pseudo-code for AUGMECON-R. Its paradigm is implemented through a $q_{\mathcal{RC}} \times q_{\mathcal{CO}}$ array, i.e., *flag*, initialised with zero values. At each iteration: if $flag[i_{\mathcal{RC}}, i_{\mathcal{CO}}] = 0$ the SOP is solved, otherwise the algorithm performs $flag[i_{\mathcal{RC}}, i_{\mathcal{CO}}]$ jumps in the innermost loop (the one relative to $\varepsilon_{\mathcal{CO}}$) (Nikas et al., 2022).

Algorithm 1 AUGMECON-R Procedure

procedure AUGMECONR ($q_{\mathcal{RC}}, q_{\mathcal{CO}}, \delta$)
  Compute the payoff table *PayTab*. ▷ Lexicographically
  Set $r_{\mathcal{RC}} = \max_{PayTab} \mathcal{RC} - \min_{PayTab} \mathcal{RC}$ and $r_{\mathcal{CO}} = \max_{PayTab}(-\mathcal{CO}) - \min_{PayTab}(-\mathcal{CO})$
  Set $step_{\mathcal{RC}} = r_{\mathcal{RC}}/(q_{\mathcal{RC}} - 1)$ and $step_{\mathcal{CO}} = r_{\mathcal{CO}}/(q_{\mathcal{CO}} - 1)$.
  Set $q = 0$, $g = 0$ and *Pareto_Set* $= \emptyset$.
  Set $b_{\mathcal{RC}} = 0, b_{\mathcal{CO}} = 0, S_{\mathcal{RC}} = 0$ and $S_{\mathcal{CO}} = 0$.
    ▷ Bypass coefficients and slack variables
  for $q < q_{\mathcal{RC}}$ and $g < q_{\mathcal{CO}}$ **do**
    $flag[q, g] = 0$
  endfor
  while $q < q_{\mathcal{RC}}$ **do**
    while $g < q_{\mathcal{CO}}$ **do**
      if $flag[q, g] == 0$ **then**
        $\varepsilon_{\mathcal{RC}} = \max_{PayTab} \mathcal{RC} - q * step_{\mathcal{RC}}$ and $\varepsilon_{\mathcal{CO}} = \max_{PayTab}(-\mathcal{CO}) - g * step_{\mathcal{CO}}$
        Pareto_Set, $S_{\mathcal{RC}}, S_{\mathcal{CO}} =$ Solve $\text{SOP}(\varepsilon_{\mathcal{RC}}, \varepsilon_{\mathcal{CO}}, \delta)$
        $b_{\mathcal{RC}} = \lfloor S_{\mathcal{RC}}/step_{\mathcal{RC}} \rfloor$ and $b_{\mathcal{CO}} = \lfloor S_{\mathcal{CO}}/step_{\mathcal{CO}} \rfloor$
        Update the flag matrix using $b_{\mathcal{RC}}$ and $b_{\mathcal{CO}}$.
          ▷ See Nikas et al. (2022)
        $g = g + 1$
      else
        $g = g + flag[q, g]$
      endif
    end while
    $q = q + 1$
  return *Pareto_Set* ▷ Pareto Set (approximation)
end procedure

Remark 2. Ideally, for each objective function, the calculation of the range would include the corresponding component of the nadir points. However, it is rather complicated to obtain these values efficiently (Isermann & Steuer, 1988). For this purpose, a well-established procedure consists in deriving the ranges from the minimum and maximum values within the payoff table obtained with the lexicographic approach (Fugaro & Sgalambro, 2023; Mavrotas, 2009; Pisacane et al., 2021) or by approximation (Fugaro & Sgalambro, 2023; Tautenhain et al., 2019). In particular, while there is no guarantee of the quality of the bounds obtained with a generic approximation approach, the use of the lexicographic method leads to an overestimation of the nadir points (Ehrgott & Tenfelde-Podehl, 2003); thus, a larger grid is obtained without affecting the quality of the (approximations of the) Pareto Sets produced (Mavrotas & Florios, 2013). ■

Appendix C

Representation of efficient solutions for the case study

This section presents the alternative configurations obtained for the various parameter settings considered in the scenario-based analysis. The order of the solutions reflects their ranking according to the OPSBC method.

In each figure, purple indicates covered cells and a blue circle depicts an active HWRC. The coverage area of each HWRC is also represented by a dashed circle. The gauges on the right correspond to the values of $\mathcal{CO}$, $\mathcal{RC}$, and $\mathcal{UC}$. The colour of the gauges ranges from green (best value) to red (worst value).

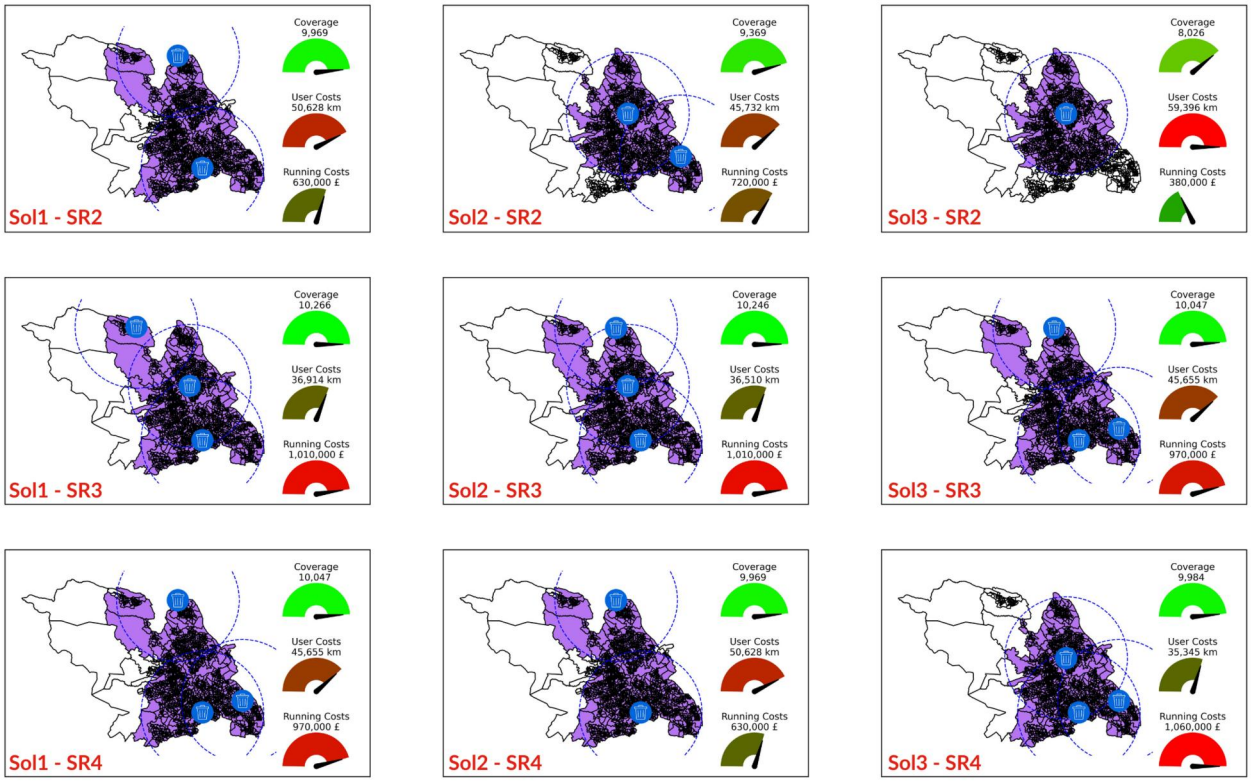

Figure C1. Solutions for the SR scenarios.

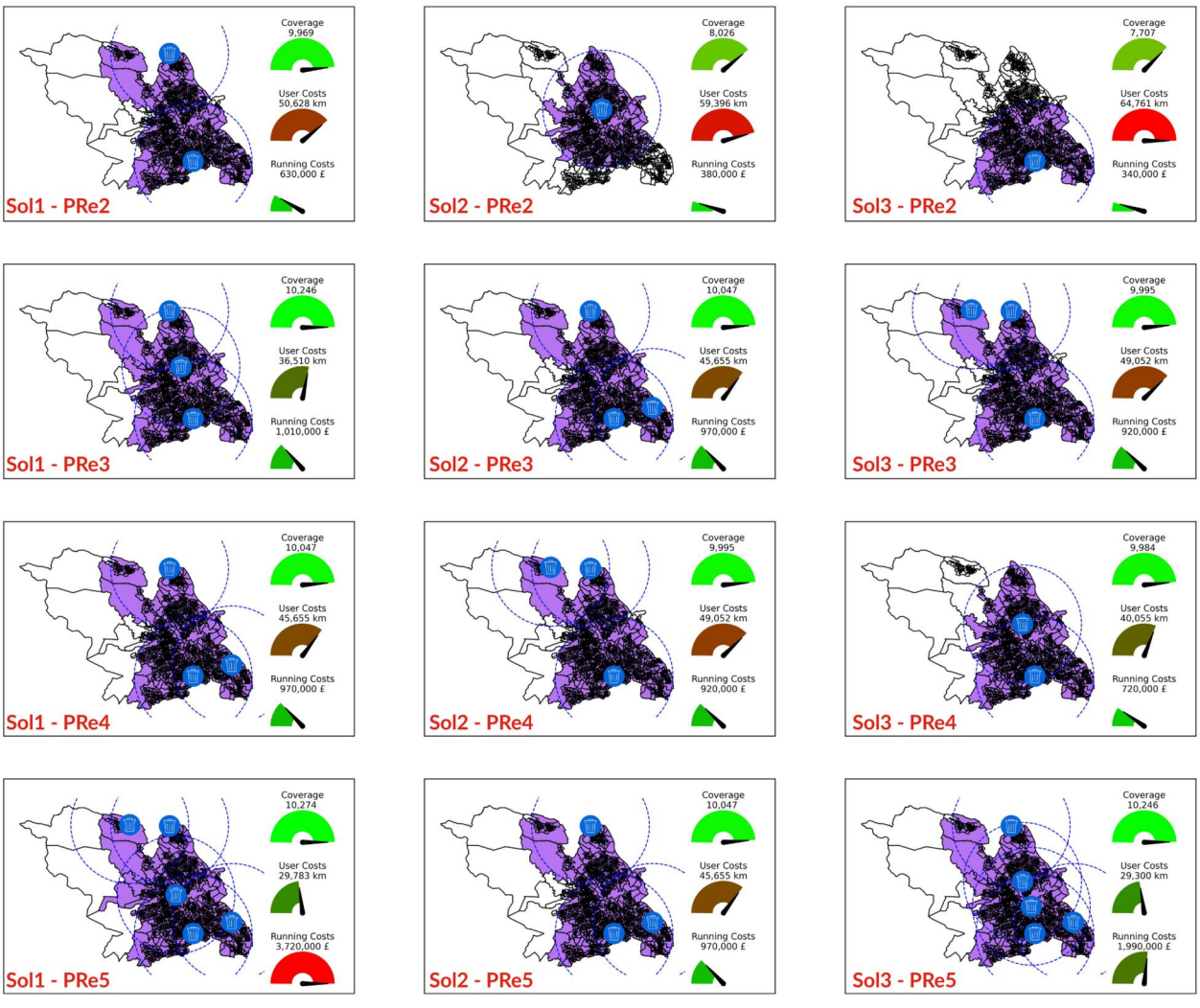

Figure C2. Solutions for the P-Re scenarios.

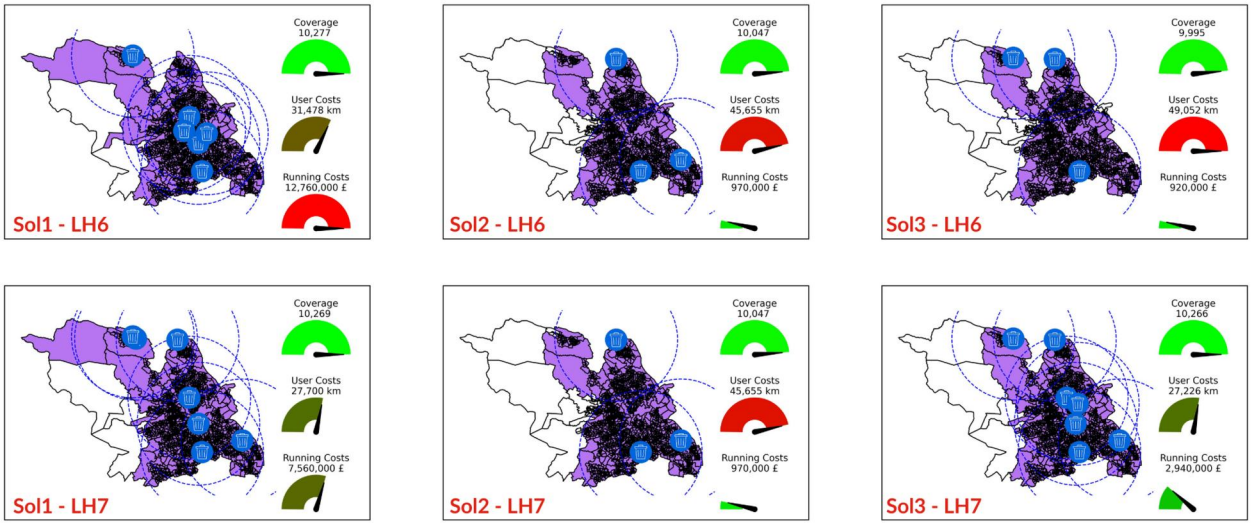

Figure C3. Solutions for the LH scenarios.

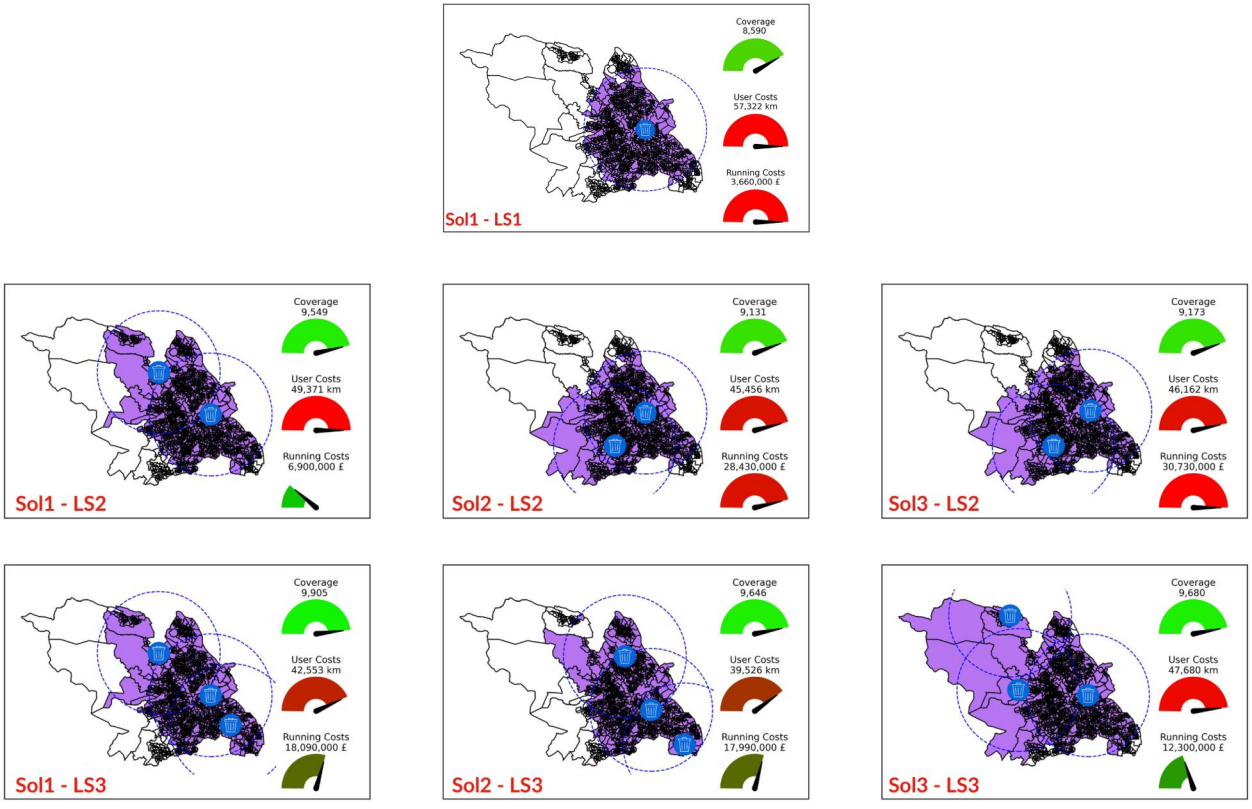

Figure C4. Solutions for the LS scenarios.

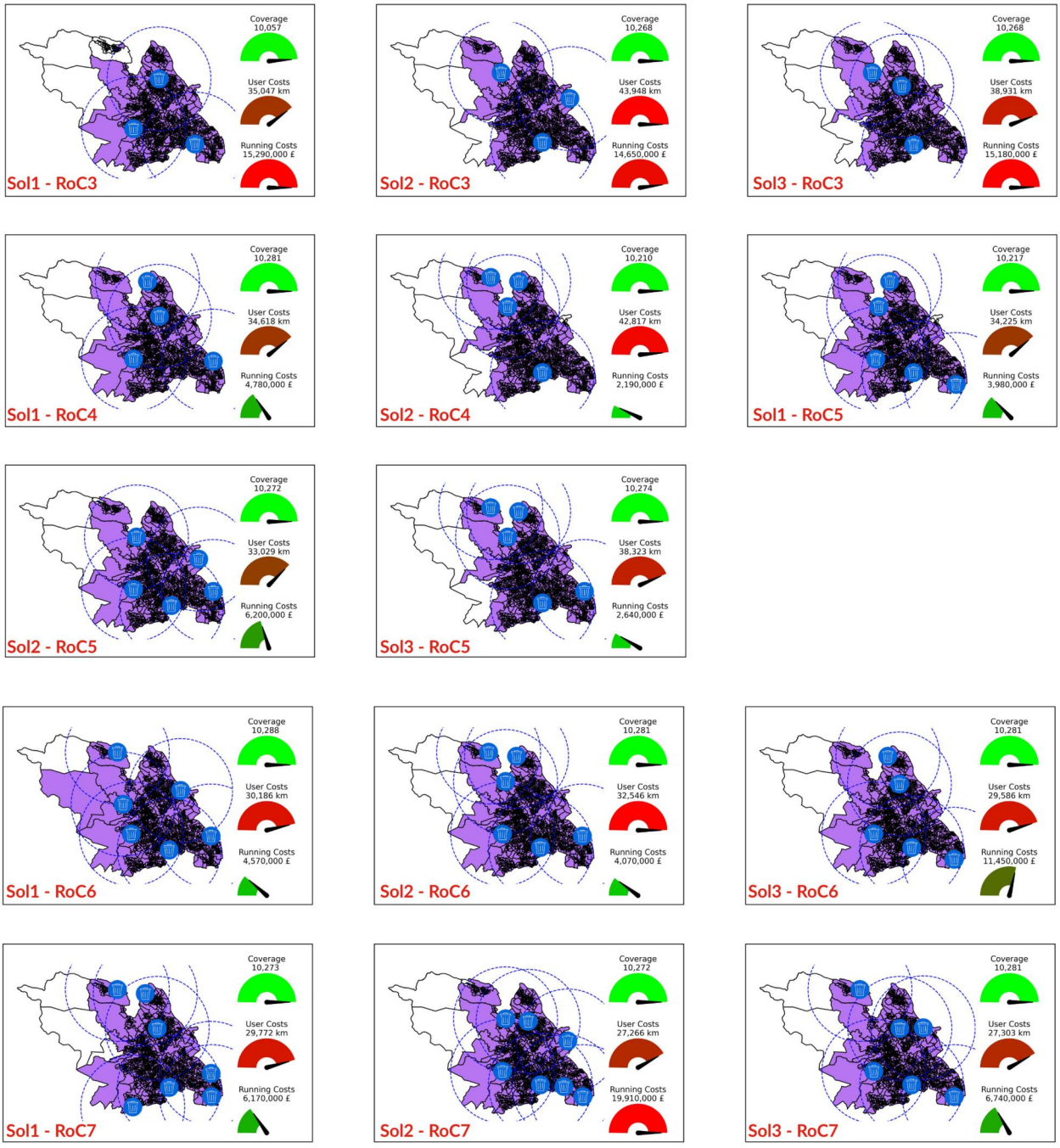

Figure C5. Solutions for the Ro-C scenarios.

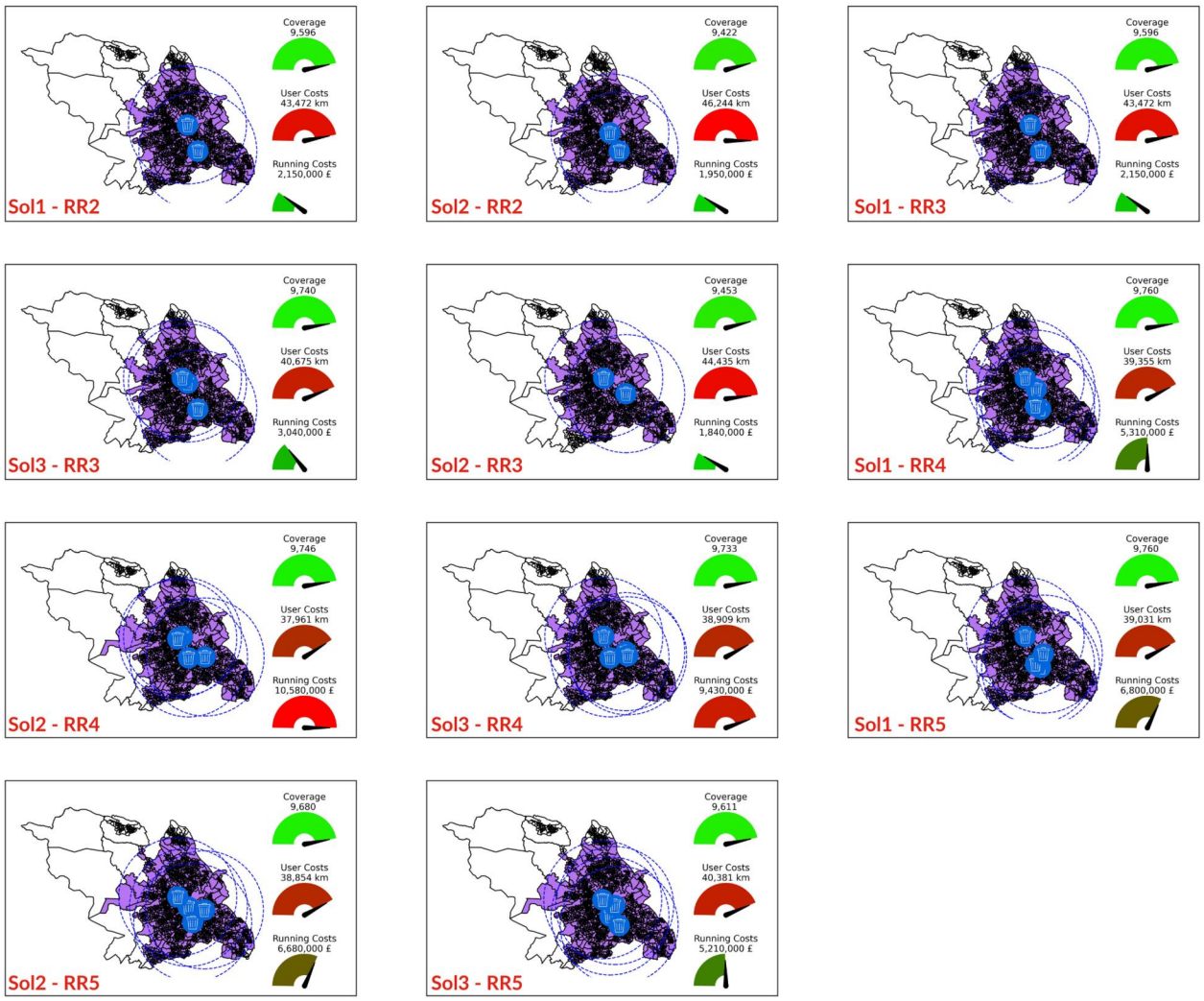

Figure C6. Solutions for the RR scenarios.